The Protective Role of Stem Cell Factor (SCF) in Regulating UV-mediated DNA damage in Amelanotic Keratinocytes

A Thesis

submitted to

Indian Institute of Science Education and Research Pune in partial fulfilment of the requirements for the BS-MS Dual Degree Programme

by

Shubham Indoriya

Indian Institute of Science Education and Research Pune

Dr. Homi Bhabha Road,

Pashan, Pune 411008, INDIA.

April, 2025

Under the guidance of

Supervisor: **Dr. Archana Singh,**

Principal Scientist at CSIR-IGIB

From May 2024 to Mar 2025

INDIAN INSTITUE OF SCIENCE EDUCATION AND RESEARCH PUNE

Certificate

This is to certify that this dissertation entitled **"The protective role of Stem Cell Factor (SCF) in regulating UV-mediated DNA damage in amelanotic keratinocytes"** towards the partial fulfilment of the BS-MS dual degree programme at the Indian Institute of Science Education and Research, Pune represents study/work carried out by **Shubham Indoriya** at **Institute of Genomics and Integrative Biology (CSIR-IGIB)** under the supervision of **Dr. Archana Singh**, Principal Scientist at Institute of Genomics and Integrative Biology during the academic year 2024-2025.

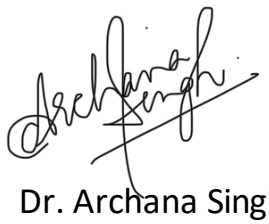

Dr. Archana Singh

Date: 26th March, 2025

TAC Committee:

Dr. Archana Singh

Dr. Vineeta Bal

This thesis is dedicated my uncle **Mr. Bhanu Prakash Sharma**

Declaration

I hereby declare that the matter embodied in the report entitled **"The protective role of Stem Cell Factor (SCF) in regulating UV-mediated DNA damage in amelanotic keratinocytes"** are the results of the work carried out by me at the Department of Biology, **Institute of Genomics and Integrative Biology (CSIR-IGIB)**, under the supervision of **Dr. Archana Singh** and the same has not been submitted elsewhere for any other degree. Wherever others contribute, every effort is made to indicate this clearly, with due reference to the literature and acknowledgement of collaborative research and discussions.

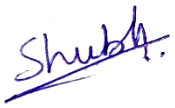

Shubham Indoriya

Date: 26th March, 2025

Table of Contents

List of Tables

List of Figures

Abbreviations

- SCF - Stem Cell Factor
- SIRT1 - Sirtuin1
- DRP1 - Dynamin Related Protein 1
- MFN1 - Mitofusin1
- ROS - Reactive Oxygen Species
- NHEK - Normal Human Epidermal Keratinocytes
- rh-SCF - recombinant human Stem Cell Factor
- CPD - Cyclobutane Pyrimidine Dimers
- LPL - lipoprotein lipase
- NL - non-lesional; L, lesional
- BCA - Bicinchoninic Acid
- BSA - Bovine Serum Albumin
- HRP- Horseradish peroxidase
- ECL - Enhanced Chemiluminescence Reagent
- EDTA - Ethylenediaminetetraacetic acid
- PAGE – Polyacrylamide Gel Electrophoresis
- PBS - Phosphate Buffered Saline
- PVDF – Polyvinylidene fluoride
- SDS – Sodium Dodecyl Sulphate
- TBST – Tris-buffered saline with 0.1% Tween 20 detergent

Contributions

Contributor name	Contributor role
Dr. Archana Singh	Conceptualization Ideas
Manish Chowdhary, Dr. Archana Singh	Methodology
Manish Chowdhary	Software
Manish Chowdhary	Validation
Shubham Indoriya, Manish Chowdhary	Formal analysis
Shubham Indoriya, Manish Chowdhary	Investigation
Manish Chowdhary, Dr. Archana Singh	Resources
Shubham Indoriya, Manish Chowdhary	Data Curation
Shubham Indoriya	Writing - original draft preparation
Shubham Indoriya, Manish Chowdhary	Writing - review and editing
Dr. Archana Singh	Visualization
Dr. Archana Singh	Supervision
Dr. Archana Singh	Project administration
CSIR	Funding acquisition

Abstract

Vitiligo, a condition characterized by loss of melanocyte and depigmentation, paradoxically associates with a lower risk of skin malignancies. This study explores the protective molecular pathways in vitiligo keratinocytes against UV-induced DNA damage. We uncover a new stem cell factor (SCF)-mediated pathway that induces lipoprotein lipase (LPL) and sirtuin 1 (SIRT1) to counteract UVB-induced cellular damage. SCF treatment decreased γ-H2AX positivity and cyclobutene pyrimidine dimer (CPD) formation strongly, enhanced the health of the mitochondria (elongated morphology, reduced reactive oxygen species and lipid peroxidation), and normalized lipid metabolism through increased LPL expression. Disruption of LPL using siRNA knockdown caused elevated DNA damage and lipid droplet formation, all effects reversed with NO-1886, a selective LPL agonist. In addition, pharmacological or genetic SIRT1 inhibition eliminates SCF-mediated protective effects, positioning SIRT1 as the critical downstream effector in the SCF-LPL- SIRT1 pathway. Vitiligo patient skin biopsy analysis supports SCF and LPL upregulation in lesional epidermis. Collectively, these discoveries identify a new SCF-LPL-SIRT1 pathway, showing that SCF-induced lipid metabolism remodeling is responsible for keratinocyte protection against UV damage and for the natural tumor suppressive milieu in vitiligo skin. These findings disclose possible therapeutic opportunities for preventing UV damage and skin cancer.

Acknowledgments

This journey has been tough but at the same time very rewarding and I wouldn't have made it to this mark without the help of some amazing people.

First and foremost, I wish to express my sincerest gratitude to Dr. Archana Singh. Your guidance, patience, and constant support have been key in developing both this research and my academic development. Thank you for believing in my potential, for pushing me to think deeply through your insightful feedback and encouragement. I am really thankful for your mentorship and for all the countless hours of discussions and I will always be grateful for the lessons you have taught me.

I express a heartfelt and special thanks to Mr. Manish Chowdhary, for your exceptional mentorship throughout the duration of this project. I am grateful for your valuable guidance, critical feedback, and constant encouragement throughout this experience. Your trust in me has been a confidence booster and inspiration, and I am grateful for the skills and knowledge that I have acquired through your guidance.

To my amazing lab mates, thank you for making this experience both stimulating and fun. The late hours in the lab, the collective struggles, and the shared triumphs have been made all the more worthwhile because of your friendship and support. Your teamwork and encouragement have fostered a spirit of learning and growth that I will always treasure.

To my Family, I cannot express how grateful to you I am for your unconditional love and support. You have been my greatest strength and motivation.

And to my wonderful friends, thank you for always cheering me on, offering a listening ear, and keeping me sane through this journey. Your belief in me means everything.

This thesis is not mine; it belongs to all of you who have supported me so far, step by step. Thank you very much.

Chapter 1: Introduction

1.1Skin

1.1.1 Introduction

Skin is the largest organ of the human body, which covers an individual's entire body. It constitutes about 15% of adult body weight. Skin is a complex system that coordinates neurosensory connections to the surrounding, protects against UV induced damage, maintaining body's biological homeostasis and the functioning of barriers including pathogen attack, environmental factors like temperature, and various biochemical and metabolic functions (Boer, 2016). In addition, the mucous membranes that border the body's surface are continuous with the skin. The skin performs several essential tasks. It provides vital defense from the environmental factors by serving as the initial physical barrier against germs, dehydration, UV rays, and mechanical injury. The skin is the first organ to register pain, warmth, touch, and deep pressure. Furthermore, the skin promotes fluid circulation of the body and is essential for endocrine function because it starts the biochemical reactions that produce Vitamin D, which is required for calcium absorption and healthy bone metabolism. Water, urea, and ammonia are released during exocrine activity, while sebum, perspiration, and pheromones are secreted as well. Important immunologic tasks are also carried out by the skin, which secretes bioactive molecules like cytokines to promote the development of immunity against infections. Additionally, the skin controls body temperature through sweat glands and blood vessel regulation. Variations in skin thickness may vary based on age, gender, location, medication, and overall health.

1.1.2 Layers of skin

The epidermis, dermis, and hypodermis are the three separate layers that make up the skin, and each has a different structure and purpose.

Keratinocytes, the cells that make up the epidermis, the outermost layer, are responsible for producing keratin, a long, thread-like protein that serves as protection. Collagen, a fibrillar structural protein, comprises most of the middle layer, or dermis. Little lobes of fat cells called

lipocytes are found in the hypodermis, or subcutaneous tissue, under the dermis. Based on the thickness of the epidermis and dermis, each skin layer is classified, with variations in thickness depending on the body area.

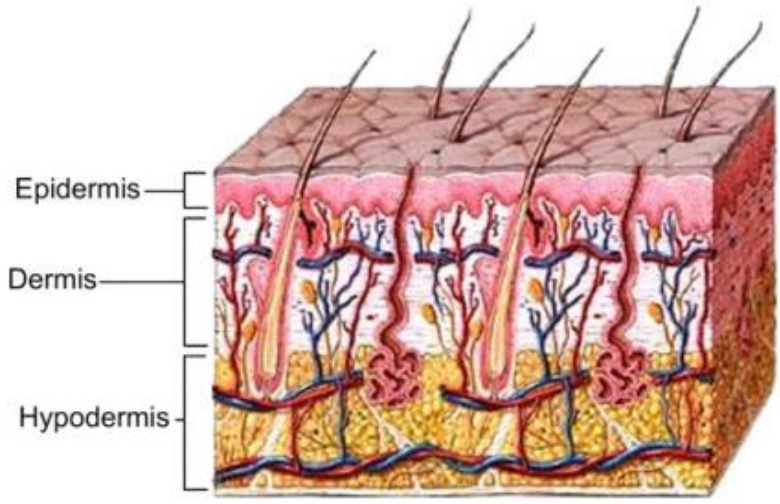

Figure 1 Skin anatomy – Layers of skin

Figure 1: Skin anatomy- Different layers of skin (Khavkin et al, 2011).

1) EPIDERMIS

The primary constituents of the stratified squamous epidermis are dendritic and keratinocyte cells. The skin's outermost layer, the epidermis, contributes to skin tone and acts as a waterproof barrier. The epidermis is a layer that continually regenerates and gives rise to derivative structures such as sweat glands, nails, and hair follicles. Keratinocytes make up the bulk of cells in the epidermis, but there are other cell types as well, such as melanocytes, Langerhans cells, and Merkel cells. Stratum basale, stratum spinosum, stratum granulosum, stratum lucidum, and stratum corneum are the five layers of the epidermis that make up thick skin, such as seen on the palms and soles. Other regions lack the stratum lucidum and have just four layers of the epidermis.

a) Stratum Basale

The thickest layer of the skin is called the stratum basale, or stratum germinativum. Hemi desmosomes attach the stratum basale to the dermis, which is separated from it by the basement

membrane (basal lamina). This layer consists of actively dividing cuboidal to columnar stem cells that continually produce keratinocytes.

b) Stratum Spinosum

There are eight to ten cell layers in the stratum spinosum, which is also referred to as the prickle cell layer. It has a polyhedral, irregular cell structure with cytoplasmic extensions, also called "spines," that extend outward and attach to other cells by desmosomes. Furthermore, dendritic cells are present in this layer.

c) Stratum Granulosum

The stratum granulosum consists of three to five layers of cells and contains diamond-shaped cells with lamellar and keratohyalin granules. Keratohyalin granules hold precursors of keratin, which eventually aggregate, crosslink, and form bundles.

d) Stratum Lucidum

Two to three cell layers make up the thin, transparent stratum lucidum. Thick skin, like that of the palms and soles, contains it. Keratohyalin undergoes a transition to produce eleidin, which is present in this layer.

e) Stratum Corneum

The topmost layer of the epidermis, known as the stratum corneum, is made up of 20–30 cell layers. It consists of horny scales consisting of dead keratinocytes, sometimes referred to as anucleate squamous cells and keratin. The thickness of this layer varies greatly, especially in callused skin. The dead keratinocytes in the stratum corneum release defensins, which are a component of our first line of defense against pathogens.
The cells of the epidermis include keratinocytes, melanocytes, Langerhans' cells, and Merkel's cells.

i. Keratinocyte

The outermost layer of the skin, known as the epidermis, is mainly made up of keratinocytes. These cells play a crucial role in forming a physical barrier to protect the body from infections, environmental damage, and dehydration. They contain abundant proteins such as keratin and keratohyalin. Keratinocytes are important for the regeneration of skin and healing procedures because of their fundamental function in building the epidermis and preserving the skin barrier.

Improvements in regenerative healthcare and dermatological therapies can be made by studying their behavior and optimizing it. Keratin creates strands of elastic fibrils extending throughout the cell to provide structure and tensile strength. Keratin filaments perpendicular to the skin's surface are present in the cytosol of the stratum basale. Keratin filaments extend in a concentric pattern around the nucleus and insert into peripheral desmosomes in the next layer, called the stratum spinosum, so called because of the "spines" that connect keratinocytes. Keratin Provides structure and tensile strength by forming bundles of elastic fibrils that stretch across the cell. Keratohyalin Granules comprise profilaggrin, a 400-kD molecule cleaved into 37-kD filaggrin peptides found in the stratum granulosum. The cornified envelope is Composed of cross-linked proteins like loricrin and involucrin and provides major protection to keratinocytes, linking intracellular keratins and extracellular lipids. Keratinocytes, the primary cell type in the epidermis, play several crucial roles beyond providing structure and strength through keratin and filaggrin. Notably, they also regulate calcium absorption by converting cholesterol precursors into vitamin D upon exposure to UVB light. Each keratinocyte is surrounded by a cornified envelope, which strengthens the skin's defense barrier by aiding in lipid and keratin attachment, protecting cells, and preventing moisture loss.

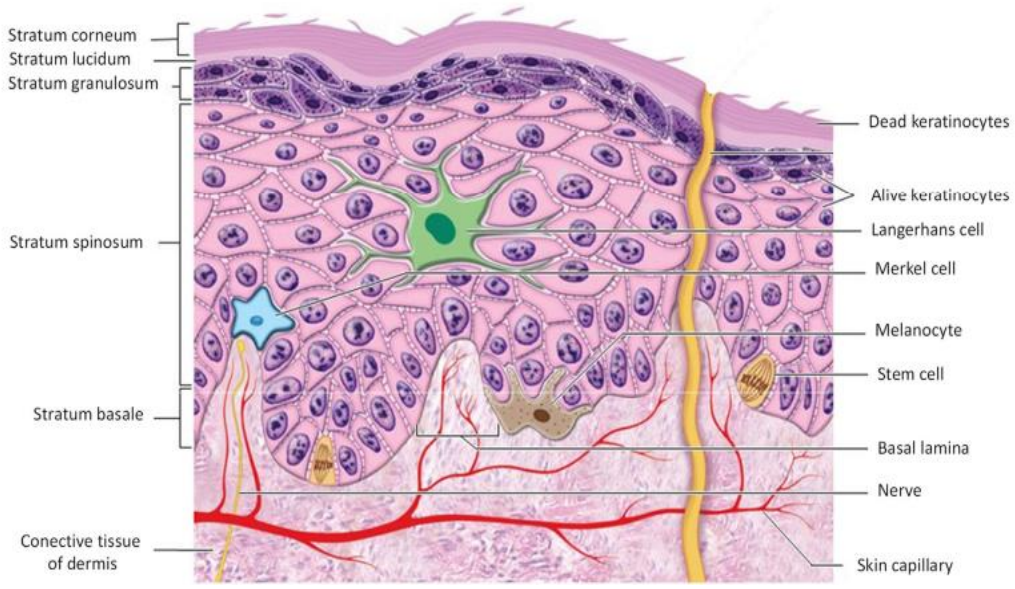

Figure 2 Cell types and sub layers of epidermis

Figure 2: Cell types and different layers of epidermis (Souto et al, 2022)

2) DERMIS

The dermis is a dense and intricate network of fibrous, flexible, and crystalline connective tissue. It nourishes neuronal and vascular networks destined to enter and appendages produced from the epidermis, such as sebaceous glands, sweat glands, and hair follicles.

Fibroblasts that synthesize collagen and other structural amino acids plus mast cells and macrophages assisting in tissue healing and immunological responses are also found in the dermis. The dermis is primarily composed of the papillary and reticular connective tissue layers, with each layer merging into one another with indistinct boundaries. It is attached to the epidermis at the junction of the basement membrane and subcutaneous fascia.

The dermis is primarily an interconnected mix of collagen fibers, whereas elastic fibers define elasticity. The dermis has higher cellularity close to the epidermis and is termed the papillary layer. The deeper, thicker, and less cellular reticular zone is collageneic and well vascularized. The thickness of the dermis varies greatly; it may only reach 1 mm on the eyelids and exceeds 5 mm on the back. It is a tough, durable covering imbued with specialized structures that protect the body from mechanical injury. At the level of the basement membrane, the dermis is connected to the epidermis and is inwardly bounded by subcutaneous fat. Collagen fibers synthesized by fibroblasts are the dominant component of dermis, collagen being its main entity. Interstitial collagen Types I and III constitute more than 90% of dermal fibers providing skin with elasticity and mechanical resistance. These elastic fibers stretch from the densa mucosa that connects the epidermal-dermal junction through the reticular dermis, allowing the skin to return to its original shape after deformation.

The dermis makes sure that the features in both the cells are maintained. These two areas work together, from embryonic development onwards, form the epidermal appendages and dermal-epidermal junction. During the healing of wounds, the two also work together to regenerate and repair the skin. All components of the dermis are mesodermal in origin while nerves arise from the neural crest and melanocytes. The dermis, until six weeks of fetal life, can be defined as a mere collection of dendritic-shaped cells containing acid mucopolysaccharides, the building material of fibroblasts (1). Elastin fibers too lie interspersed within the dermis adding some degree of elasticity to the skin (7).

3) HYPODERMIS

The hypodermis, also known as subcutaneous fascia, is situated deep to the dermis. Adipose lobules together with other skin appendages such as hair follicles, sensory neurons, and blood vessels are found in this lowermost layer of the dermis. The hypodermis is an essential layer of skin that helps with insulation that regulates body temperature, protection, storage of energy. Structurally, the hypodermis consists predominantly of adipocytes arranged in lobules. These lobules are demarcated by connective tissue septae which provide mechanical support and compartmentalize the adipose tissue.

Adipocytes within this layer store lipids, which can be metabolized to release energy during periods of increased demand or nutritional deficiency. Its structure and thickness vary based on anatomical location, individual genetics, and nutritional status. The hypodermis varies in thickness across different bodily sections. For example, in regions like the belly, thighs, and buttocks, the layer is often thicker. The hypodermis's thickness can be influenced by lifestyle decisions and genetics. A person's dietary state is indicated by the quantity of fat that is stored in the hypodermis. The hypodermis of well-nourished persons who are healthy is usually thicker than that of undernourished people.

Keratinocytes, melanocytes and fibroblast are associated in a complex relationship which combines signaling mediated by substances released into cells with direct cell-to-cell contact. In order to maintain appropriate cellular configuration and function within the skin, keratinocytes engage in extensive molecular interactions across nearby cells to construct an elaborate network defined as the "interactome." This cross-talk governs the biological functioning, survival, modulate pigmentation while preserving tissue integrity. It controls the proliferation of melanocytes as well as responses to external stimuli like UV-damage (T., 2005).

1.2 Environmental stress factors inducing DNA Damage in skin

In addition to providing protection, the skin acts as an evolving connection with the environmental stimuli. Skin comes in contact with numerous conditions every day like temperature fluctuations, allergens, volatile chemical substances, sunlight, UV-radiations, which in turn causes dehydration, allergic reactions, inflammation, dryness, and pigmentation in the skin. Dry or oily skin disorders can be caused by imbalances in the lipid content of the

skin as a result of environmental influences. Skin irritation by chemicals or physical agents can result in dry, pigmented, cracked, or sensitive skin. Reactive skin is characterised by tingling sensations inflammation, and sensory complaints. Physical, pharmacological, psychological, or hormonal reasons can cause reactive skin. When exposed to certain substances, immunological responses to allergens can include vesicles, erythema, eczema, and pruritus (Misery, 2007) (Landau, 2007).

While environmental variables like UV exposure may accelerate up skin pigmentation through intricate biochemical pathways encompassing DNA damage, collagen breakdown, and inflammatory processes, genetic alterations are foreseeable and gradual. To prevent skin pigmentation and preserve skin health throughout time, it is essential to comprehend these processes and devise approaches effectively. Targeted techniques in conjunction with protection from UV rays and other environmental triggers can help maintain skin function and integrity as people get older (D'Orazio J, 2013).

Based upon its origin, skin DNA damage can be divided into two primary classes: endogenous and exogenous. The vast majority of endogenous DNA damage results from chemically active DNA interacting with water in addition ROS, which are naturally occurring in cells, in hydrolytic and oxidative ways, respectively. Hereditary conditions and spontaneous cancers are caused by these naturally occurring predisposing interactions of DNA with chemicals from

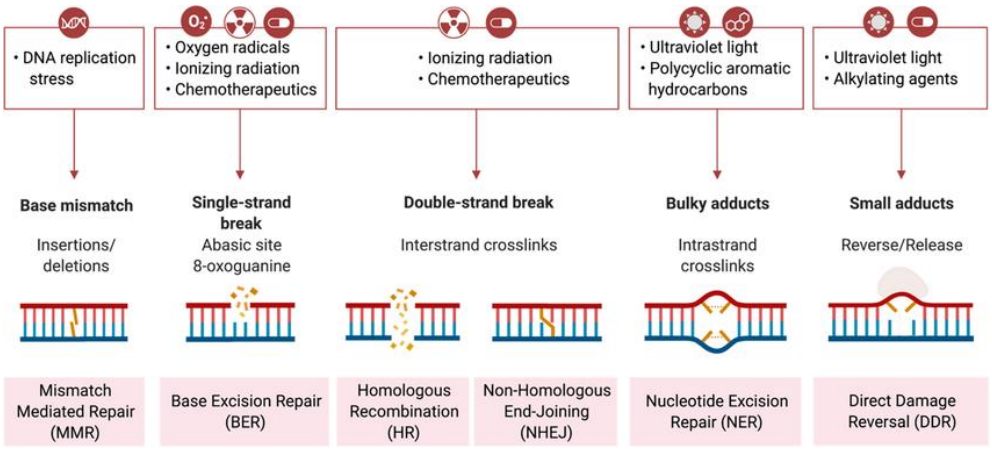

Figure 3 DNA damage factors and mechanisms

Figure 3: DNA damage causes and response mechanisms (Hendi, The base excision repair process: comparison between higher and lower eukaryotes., 2021)

its vicinity. However, exogenous DNA damage happens when the DNA is harmed by environmental factors. A few conditions are ionizing radiation (IR) and UV-rays, alkylating chemicals, and crosslinking agents (Chatterjee, 2017).

UV-induced DNA damage, pigmentation and aging has become a widely researched area. UV radiations comprise of a spectrum consisting of UV-A (range 315-400nm), UV-B (range 280-315nm), UV-C (range 100-280nm). The variations are due to differences in energy levels and wavelength of sunlight. DNA damage is a consequence of UV-B rays whereas UV-A causes maturation and ROS accumulation i.e., oxidative stress in the body.

DNA damage occurs at targeted sites in the DNA at the dipyrimidine sites which cleaves intrinsic interactions within pyrimidine bases to modify the chemical composition of nucleotide bases A and T nucleotide resulting in dimer formation. Majorly photoproducts including pyrimidine (6,4)- pyrimidone photoproducts (6-4PPs) and cyclobutane pyrimidine dimers (CPDs) are generated, which alter the cellular structure of DNA and obstruct fundamental biological functions like transcriptional activities and DNA replication. These lesions can lead to the emergence of skin cancer and are extremely mutagenic (Giglia-Mari). CPDs occurrence is commonly found between thymine (T) base pairs which are covalently bonded to one another. These lesions cause formation of cyclobutane ring like structures which breaks the bonds and disrupts the helix leading to inhibition of transcription. 6-4PPPs inhibits DNA replication and transcription using the same mechanism as CPDs, wherein within the same DNA strand, a covalent link forms connecting carbon atoms at positions 6 and 4 of contiguous pyrimidine bases, such as cytosine (C) or thymine (T) causing DNA helix disruption. These lesions are the underlying cause of mutations and carcinoma. Skin responses to environmental stimuli, like those observed from stress, can be influenced by sensory and psychological perceptions. As a result, the environment can alter skin characteristics in a broad range.

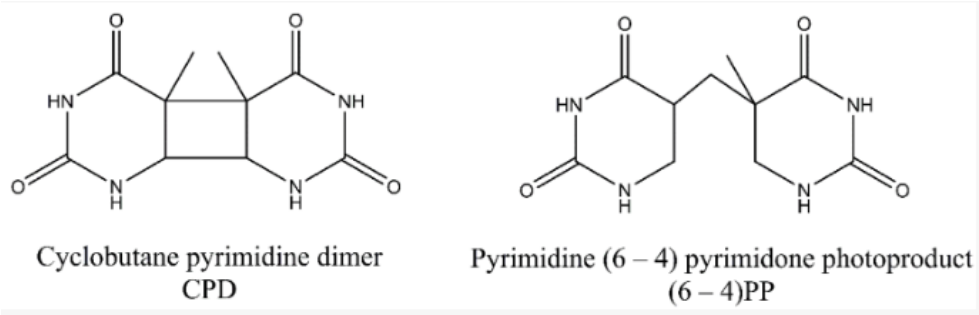

Figure 4 UV-B induced Photo-products

Figure 4: UV- induced DNA damage photoproducts CPD and 6-4PP (Kciuk M, 2020)

1.3 DNA Damage Repair

To combat UV-induced DNA damage, cells have developed networks to identify DNA lesions, indicate their existence, and facilitate their repair. These systems are collectively referred to as DNA-damage response (DDR). These processes of DNA repair can be grouped into two categories: One through direct reversal of the chemical process that has caused DNA damage, and through excision of the damaged bases followed by their replacement with new DNA synthesized (Hendi, 2021).

Photoreactivation is a process for direct reversal of DNA damage which utilizes Photolyases are specialised enzymes that repair DNA which have the ability to directly reverse the process by which UV light forms cyclobutane pyrimidine dimers. Photolyase enzymes undergo a conformational change in their active site upon binding to DNA that contains CPDs. The photolyase enzyme is activated by the absorbed photon energy, which permits it to disassemble the cyclobutane ring structure inside the pyrimidine dimer. The DNA sequence is restored when photolyase breaks the ring, enzymatically separating the covalently bound pyrimidines back into their constituent bases.

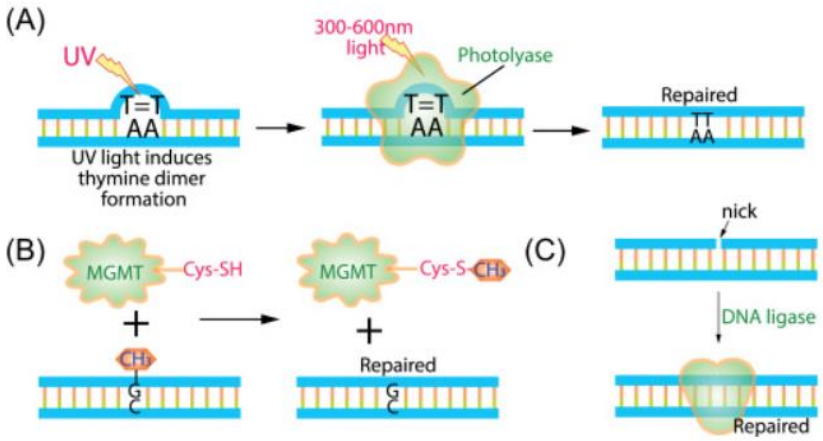

Figure 5 Direct reversal of DNA damage

Figure 5: Direct reversal of DNA damage in CPD and 6-4PP using photolyase and MGMT mechanisms (Bhagavan, DNA Replication, Repair, and Mutagenesis, 2002)

Another mechanism uses MGMT- O6-methylguanine methyltransferase for repairing DNA damage caused by alkyl agents like alkyl nitrosoureas, dialkyl nitrosamine, acyl nitrosamides.

Guanine (G) bases have the ability to methylate at the O6 location when exposed to alkyl compounds, creating O6-methylguanine. The DNA repair enzyme MGMT has an unique ability to identify and modify O6-methylguanine defects. In order to reverse the chemical changes, the enzyme directly transfers the methyl group from the methylated G base's O6 position to a C residue inside its active site, restoring the original G bases and normal DNA structure (Yu, 2020) (Bhagavan, 2002).

One essential part of the cellular DDR system that maintains genomic integrity is the process of DNA double-strand break (DSB) repair. Ionizing radiation, such as gamma rays, X-rays, and internal radiation from radioactive materials within the Earth causes DSBs since they produce free radicals detrimental to DNA. DSBs are extremely cytotoxic lesions that may cause genetic instability if not repaired or are repaired incorrectly. To identify, signal, and repair DSBs, the DDR uses a complicated web of molecular processes coordinated by multiple proteins and pathways. Cellular sensors, such as the MRN (MRE11-RAD50-NBS1) complex, possess the ability to detect double-strand breaks (DSBs) promptly recruit ATM (ataxia-telangiectasia mutated) kinase to the damage site. When serine kinase ATM is activated, a signaling cascade is set off, which phosphorylates many substrates and initiates checkpoints at the G1/S, intra-S, and G2/M phases in cell cycle that hinders the cell cycle from continuing and aiding in DNA repair. Histone H2AX is phosphorylated at serine 139 by ATM kinase, resulting in γH2AX, a crucial indicator of double-strand breaks. γH2AX facilitates the building of repair complexes by recruiting more ATM kinase to damage site. Repair mechanisms used are homologous recombination (HR) and Non-homologous end joining (NHEJ). ATM is essential for controlling these repair processes.

1.4 Role of Melanin

Melanocytes consist of intracellular membrane bound organelles known as melanosomes. These organelles are responsible for the production of melanin causes skin pigmentation in individuals. Tyrosinase family proteins are involved in the enzymatic production of melanin called melanogenesis. Within melanosomes, these proteins convert the amino acid tyrosine. Tyrosinase has a significant impact on the expression of melanogenic glycoproteins through its interactions with TYRP1 and TYRP2(DCT). In order to form a stable complex with tyrosinase during melanin formation, TYRP1, the most abundant melanosomal protein in

melanocytes, stabilises the melanosomal membrane. Tyrosine is converted to eumelanin using the intermediary molecule L-3,4-dihydroxyphenylalanine- L-DOPA. L-DOPA is oxidised to dopaquinone which then proceeds through a sequence of processes resulting in eumelanin. Intermediates of indole-5,6-quinone are involved in the polymerization process (D'Alba, 2019). It provides more photoprotection as compared to the reddish yellow pheomelanin which is a sub kind of melanin that has a reddish-yellow appearance. It also adds to the color of lips and nipples. It is the cause of the lighter pigmentation seen in red hair and freckles (Wasmeier, 2008)

The lesser-known and more varied class of melanin known as allomelanins is mostly present in plants, fungi, and certain invertebrates. Tyrosine is not the source of allomelanins, unlike eumelanin and pheomelanin. They are made from a variety of precursors, including indolic and phenolic chemicals, catechol, and 1,8-dihydroxy naphthalene (DHN). It synthesis pigments that are similar to eumelanin, ranging in color from dark brown to black, albeit the precise color depends on the particular precursor molecules (Ebanks, 2009)

Each melanocyte interacts with keratinocytes and transfers the melanosomes to the skin for protection against UV damage. The steady, mutually beneficial connection between keratinocytes and melanosomes is known as the Epidermal Melanin Unit (EMU). A number of diseases connected to pigmentation can result from changes made to the EMU. Melanoblasts, the precursors of melanocytes, migrate and settle in the basal layer of the epidermis by taking the dorsolateral pathway. It's noteworthy to note that unique genetic variants like receptor tyrosine kinase KIT, endothelin receptor B EDNBR, and endothelin 3 EDN3 have been connected to differences in coat color in rodents and other animals, offering insights into the genes influencing the maturation of melanocytes. Reactive oxygen species, brought on by genotoxic stressors, and adrenaline by pain, contribute to hair greying (D'Mello, 2016) (Otręba, 2013)

Dendritic extensions of melanocytes end in filopodia, which are tiny projections that resemble fingers. Pigment globules (PG) form inside these filopodia. Membrane-bound structures known as PG are inhabited by numerous melanosomes as well as a limited number of mitochondria. The packing and preparation of melanosomes for transportation is ensured by the development of PG amid the filopodia. After forming, the PG is discharged into the extracellular space from different melanocyte dendritic regions. PG separates itself from the melanocyte membrane during this releasing phase. The keratinocyte microvilli then take up the released PG.

Keratinocytes have tiny, finger-like projections called microvilli on their surface, which expand the surface area available for contact and absorption. The protease-activated receptor-2 (PAR-2) is required for the uptake and integration of PG into keratinocytes. One receptor, PAR-2, is known to be involved in the control of pigmentation among other cellular functions. Keratinocytes internalize the membrane-surrounded PG after they have been captured. The PG membrane breaks down, releasing the individual melanosomes into the cytoplasm of the keratinocyte. Individual melanosomes migrate inside keratinocytes after becoming free in the cytoplasm. They proceed in the direction of the perinuclear area, which encircles the cell nucleus. This placement affects how pigment is distributed within cell membranes and affects the skin's overall coloring (Le, Melanosome Biogenesis in the Pigmentation of Mammalian Skin, 2021)

The microphthalmia-associated transcription factor (MITF) plays a key role in controlling the expression of important melanogenic enzymes. MITF's activity is dependent on factors like the α-melanocyte stimulating hormone (α-MSH)/melanocortin 1 receptor (MC1R) pathway, which activates signaling pathways that as a result promotes the melanogenic gene expression. When α-MSH binds to MC1R, it prompts adenylate cyclase and increases the levels of cAMP. Then this cAMP is responsible for the activation of the protein kinase A (PKA) and mitogen-activated protein kinase (MAPK) pathways, which instigates the expression of MITF and downstream of the melanogenic genes (Hida, 2020) (Le, Melanosome Biogenesis in the Pigmentation of Mammalian Skin, 2021) (Suzukawa, 2012)

1.5 Vitiligo: Overview

Vitiligo is a chronic skin disorder that leads to patches of skin losing their color and becoming white or depigmented. This is caused by the destruction or malfunction of melanocytes, the cells that produce melanin-the pigment that colors the skin, hair, and eyes. It has a global prevalence of 1-2% (Teulings, Overkamp et al. 2013). Although vitiligo is not a life-threatening condition or physically aching, it is a disorder that can impact a person on an emotional and psychological level, particularly in communities where the look of one's skin is crucial to self-concept and interpersonal relationships. It occurs in people of all races and ethnic groups. Vitiligo may emerge at any time but usually happens prior to the age of 30, although some may start as early as childhood. Although many studies have been conducted, the exact etiology of

vitiligo is still not entirely clear. Yet a number of causes, which involve genetics, autoimmunity, oxidative stress, and environmental triggers, are thought to contribute significantly to its onset.

The most recognizable sign of vitiligo is the development of patches of white on the skin. The patches may be more easily seen in individuals with darker complexion because of the contrast between affected and unaffected areas. Vitiligo usually starts on parts of the body that are exposed to the sun most often, including the face, hands, arms, and feet, but it may also occur around body orifices, including the eyes, nose, mouth, and genitals. Vitiligo may also occur in hair follicles, resulting in premature whitening of scalp hair, eyebrows, eyelashes, and beard. Individuals might also suffer from depigmentation of the mucous membranes, for example, within the mouth. The development of vitiligo differs from individual to individual—some have slow and focal depigmentation, whereas others develop rapidly spreading or widespread depigmentation all over their body.

Vitiligo is divided into various types depending on the extent and distribution of the depigmented lesions. Non-segmental vitiligo (NSV), or generalized vitiligo, is the most common type and tends to be symmetrical, i.e., it occurs on both sides of the body. It is also progressive, meaning it can spread further over a period of time. Segmental vitiligo (SV), however, is localized to a single region of the body and typically follows a predictable pattern along the nerves of the skin. This form typically occurs earlier in life and tends to be more stable than non-segmental vitiligo. Focal vitiligo is a rarer type in which only a few small areas occur without extending further. Universal vitiligo, the most uncommon form, causes almost total loss of pigment all over the body.

1.4.1 Cause of Vitiligo

The exact etiology of vitiligo is still not known, although studies indicate a multifactorial pathogenesis of genetic susceptibility, dysfunction of the immune system, oxidative stress, and environmental triggers (Jin et al., 2012; Picardo et al., 2015). While the autoimmune hypothesis remains the dominant explanation for the demise of melanocytes, new evidence points out that oxidative stress and genetic susceptibility play an essential role in the onset and development of this disease. (Xie et al., 2016).

1.4.1.1 Autoimmune Mechanisms and T-Cell-Mediated Melanocyte Destruction

One of the most prominent lines of evidence in support of the autoimmune theory of vitiligo comes from the frequent association of this disease with other organ-specific autoimmune disorders, such as Hashimoto's thyroiditis, type 1 diabetes, rheumatoid arthritis, and systemic lupus erythematosus (Harris, 2017; Alikhan et al., 2011). Genome-wide association studies (GWAS) have identified several immune-related genetic loci involved in association with vitiligo, especially within the HLA (human leukocyte antigen) complex that mediates antigen presentation and immune regulation to a greater extent (Jin et al., 2012).

At the cellular level, increased autoreactive cytotoxic CD8+ T cells infiltrate the vitiliginous skin lesions and induce melanocyte apoptosis through perforin and granzyme B release in vitiligo patients (Wang & Xing, 2020; Harris, 2017). The overexpression of chemokines induced by IFN-G signaling via the JAK-STAT pathway attracts CD8+ T cells into the skin and worsens the melanocyte destruction (Richmond et al., 2017; Wang & Xing, 2020). Regulatory T cells (Tregs), which usually inhibit autoimmune responses, are dysfunctional or reduced in vitiligo patients, which leads to immunological attack upon melanocytes (Harris, 2017).

1.4.1.2 Genetic Susceptibility and Hereditary Factors

The genetic background accounts for high heritability of vitiligo, as studies showed that first-degree relatives of afflicted individuals have a risk that ranges from 10% to 30% to develop the disease themselves (Jin et al., 2012). Thousands of immune-associated genetic loci have been identified by GWAS on vitiligo; a few of these include genes regulating the immune system (HLA, PTPN22, FOXP3, IL2RA), melanocyte function (TYR, MC1R, MITF, PMEL) and oxidative stress response (CAT, GPX1) (Spritz, 2013; Richmond et al., 2017).

Associated polymorphisms of PTPN22 (protein tyrosine phosphatase, non-receptor type 22), a T-cell activation-regulatory gene have been documented in association with many autoimmune diseases including vitiligo (Jin et al., 2012). Furthermore, mutations in TYR (tyrosinase), a key enzyme in melanin synthesis, imply that abnormal melanogenesis could render melanocytes vulnerable to immune-mediated destruction (Xie et al., 2016).

1.4.1.3 Oxidative Stress and Melanocyte Susceptibility

Oxidative stress is a key instigator of vitiligo onset, as melanocytes in vitiligo patients exhibit diminished ability to detoxify reactive oxygen species (ROS) (Dell'Anna et al., 2010; Xie et al., 2016). Investigations revealed that vitiliginous skin is deficient in antioxidant enzymes, including catalase (CAT), glutathione peroxidase (GPX), and superoxide dismutase (SOD), giving rise to hydrogen peroxide (H_2O_2) accumulation (Meyskens et al., 1999). High levels of H_2O_2 not only disrupt mitochondria but also inhibit tyrosinase activity so that melanin synthesis is impaired (Xie et al., 2016).

Oxidative stress also contributes to ER stress and the concomitant activation of UPR culminating in melanocyte apoptosis (Xie et al., 2016). On the other hand, oxidative damage can promote the upregulation of HSP70, which further intensifies autoimmune reactions against melanocytes.

1.4.1.4 Environmental Triggers and Melanocyte Damage

Ultraviolet radiation, skin trauma, chemical intakes, and infections can also incite or aggravate vitiligo by causing stress to the melanocytes (Alikhan et al., 2011). In fact, sunburn-mediated inflammation when inflicted on skin could enhance immune activation against melanocytes, while other detrimental agents such as phenolic compounds from hair dyes and industrial chemicals initiate oxidative stress and thus promote melanocyte apoptosis (Xie et al., 2016).

Viral infections and bacterial infections, activating innate immune responses and pro-inflammatory releases of cytokines, further elicit response mechanisms against melanocyte destruction, have also been classified among environmental triggers of vitiligo.

Although vitiligo has no definite cure, there are many treatment options available to help manage the condition and increase skin pigmentation. Among the topical treatment are corticosteroids and calcineurin inhibitors that are generally prescribed to minimize inflammation and stimulate repigmentation. Light-based therapies such as narrowband UVB phototherapy and PUVA therapy (psoralen plus UVA light) have been found to be efficacious in the induction of the synthesis of melanin. For patients with generalized vitiligo, depigmentation therapy that involves the lightening of the remaining normal skin to match the

depigmented patches may be an option. Surgical methods such as skin grafting and melanocyte transplantation are available for stable vitiligo patients who want a permanent solution.

1.6 Stem Cell Factor (SCF)

Stem Cell Factor (SCF) or mast cell growth factor, steel factor (SLF), or Kit ligand (KL) is a key cytokine that plays significant roles in controlling hematopoiesis, melanogenesis, gametogenesis, and tissue regeneration. It is mainly active in binding to its receptor, c-KIT, a transmembrane tyrosine kinase receptor encoded by the KIT gene (Lennartsson & Rönnstrand, 2012). SCF occurs in two bioactive isoforms—membrane-bound and soluble SCF, both of which have different roles in different physiological settings (Ashman, 1999). The membrane-bound SCF is responsible for continuous c-KIT activation, while the soluble SCF is involved in short-term signaling required for cellular survival and proliferation (Rothschild et al., 2001).

The c-KIT receptor, a proto-oncogene, presents the type III receptor tyrosine kinase (RTK) family, which also includes receptors such as platelet-derived growth factor receptor (PDGFR) and colony-stimulating factor receptor (CSFR) (Roskoski, 2005). This RTK, whose primary function is hematopoietic and reproductive cell differentiation, includes hematopoietic stem cells (HSCs), melanocytes, germ cells, mast cells, and interstitial cells of Cajal (Edling & Hallberg, 2007). c-KIT auto phosphorylates its multiple tyrosine residues when bound to SCF and thus acts to recruit downstream signal transduction molecules responsible for cell proliferation, differentiation, migration, and survival (Mol et al., 2003).

In melanocyte biology, the SCF/c-KIT interaction is crucial, as mutations in the KIT gene result in piebaldism, a hereditary condition leading to abnormal and incomplete skin and hair pigmentation, due to defective migration and survival of melanocytes (Spritz, 1999). In addition, aberrant rose c-kits, a class of mutations endowed with mutations in KIT within the gastrointestinal cancers, mastocytoses, and melanomas, are thought to be associated with unregulated cell proliferation and survival (Hirota et al., 1998). In hematopoiesis, SCF plays a phenomenal role regarding self-renewal and differentiation of hematopoietic stem cells (HSCs) to ensure proper blood cell formation and immune functions.

1.4.2 Downstream Signaling Pathway of SCF-cKIT

Upon SCF binding, cKIT dimerizes and will undergo autophosphorylation at multiple tyrosines within the intracellular domain. This phosphorylation will serve as a docking site for a battery of intracellular signaling molecules for generating a range of downstream pathways related to cell survival, proliferation, and DNA repair (Mol et al., 2003).

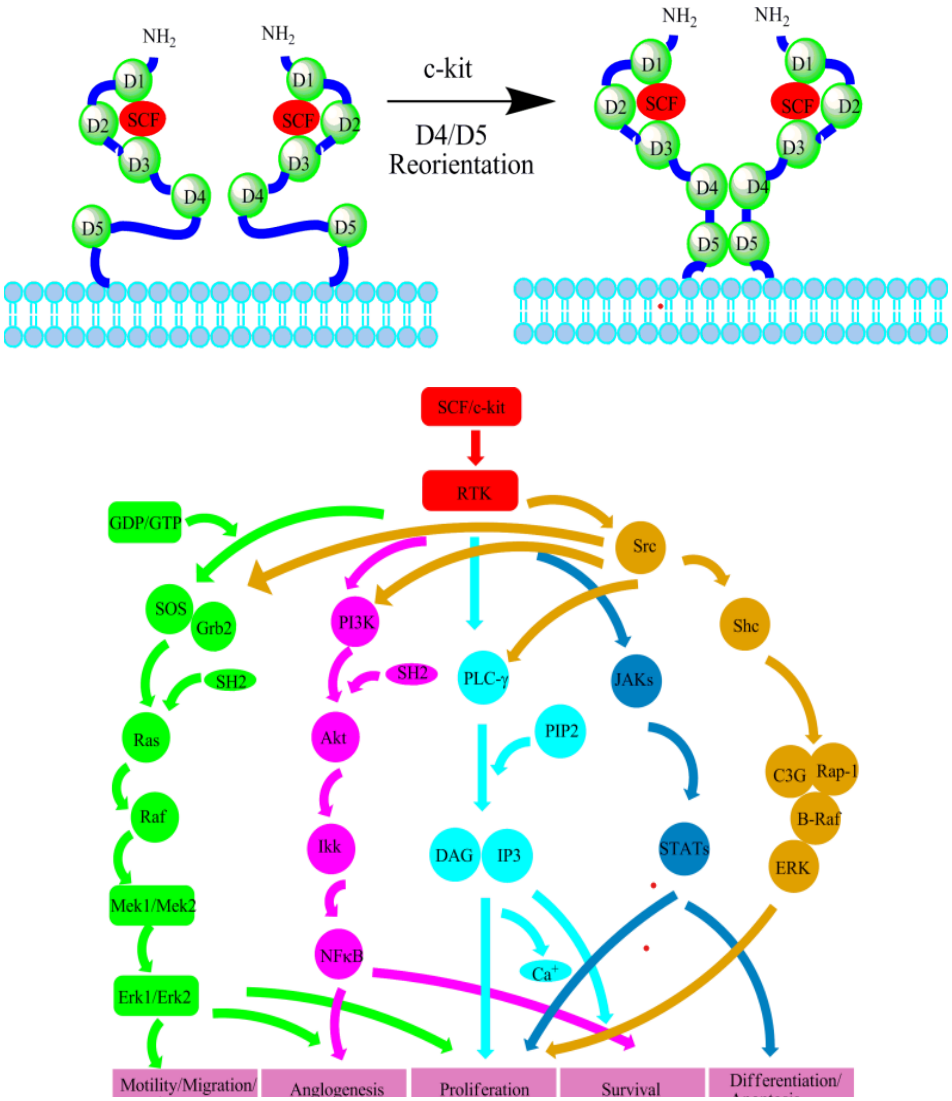

Figure 6 SCF-cKIT Downstream pathways

Figure 6: SCF-cKIT downstream pathways (J Liang, 2013)

1.4.2.1 PI3K-AKT Pathway: Central to Keratinocyte Survival

The phosphoinositide 3-kinase (PI3K)-AKT signaling pathway is among the major survival pathways mediated by SCF-cKIT signaling. cKIT activation recruits and phosphorylates PI3K, resulting in the synthesis of phosphatidylinositol-3,4,5-triphosphate (PIP3). The secondary

messenger activates AKT (Protein Kinase B), which phosphorylates various downstream effectors that are involved in cell survival and the inhibition of apoptosis (Caruana & Sukhdeo, 2021). AKT phosphorylates and suppresses pro-apoptotic proteins including BAD and caspase-9, hence preventing programmed cell death.

PI3K-AKT signaling is necessary in keratinocytes for prevention against apoptosis by UV light, maintaining epidermal integrity, and resilience against environmental insults (Jian et al., 2014).

1.4.2.2 MAPK/ERK Pathway: Promoting Cell Proliferation and Migration

Another important signaling pathway triggered by SCF-cKIT binding is the mitogen-activated protein kinase (MAPK)/extracellular signal-regulated kinase (ERK) pathway. This pathway induces keratinocyte proliferation, differentiation, and migration, all of which are important in wound healing and epidermal renewal (Lennartsson & Rönnstrand, 2012). c-KIT phosphorylation activates RAS, which in turn activates RAF, MEK1/2, and ERK1/2. Then ERK1/2 moves to the nucleus where it promotes the transcription of genes involved in cell cycle progression such as cyclin D1 (Mol et al., 2003).

ERK signaling is critical for keratinocyte migration during wound repair so that rapid re-epithelialization can be achieved (Jian et al., 2014).

1.4.2.3 The JAK-STAT Pathway: Regulation of Immune Responses

The Janus kinase (JAK)-signal transducer and activator of transcription (STAT) pathway becomes activated when the c-KIT interacts with SCF. The importance of this pathway to keratinocytes lies with immune function, cell survival, and inflammatory responses (Zhang et al. 2018). The activation of c-KIT by SCF leads to the phosphorylation of JAK1 and JAK2, which in turn phosphorylate STAT3. STAT3 enters the nucleus, where it regulates genes that promote cell survival, anti-apoptotic responses, and the expression of cytokines (Caruana & Sukhdeo, 2021).

STAT3's activation in particular is important in immune responses mediated by keratinocytes, which contribute to skin barrier maintenance and wound healing.

1.7 Sirtuin Family

Sirtuin also known as SIRT are HDAC (class III histone deacetylases) which belong to SIR2 (Silent information regulator 2) protein family tree of *Saccharomyces cervisiae*. They are NAD+ (Nicotine adenine dinucleotide+) dependent histone deacetylases which promotes deacetylation of lysine on various proteins (Grabowska, 2017).

There are 2 bilobed. globular domains in the catalytic core which have about 270 amino acids residues. The core contains an open α/β Rossmann-fold structure comprising of parallel β-sheet binding fold and Zinc Ribbon motif for protein stability. These structures form a pocket like structure for deacetylation to occur. During deacetylation, these acetyl groups get transferred to NAD+ molecule, which is facilitated by SIRT's catalytic core domain. Following the transfer, 2′-O-acetyl-ADP-ribose is released along with Nicotinamide Moreover, it functions as a noncompetitive sirtuin inhibitor via a process of base-exchange, it hinders the enzyme by interacting with a catalytic intermediate to reconstruct β-NAD+, which is the oxidised form of NAD+, at the expense of the deacetylation (Vassilopoulos, 2011). SIRTs are known to play important roles in keeping cellular processes such as inflammation, oxidative stress, DNA damage repair, apoptosis, proliferation, autophagy, and cancer under check (Yuan, 2012). Mammalian Sirtuin has 7 homologs SIRT1, SIRT2, SIRT3, SIRT4, SIRT5, SIRT6, and SIRT7.

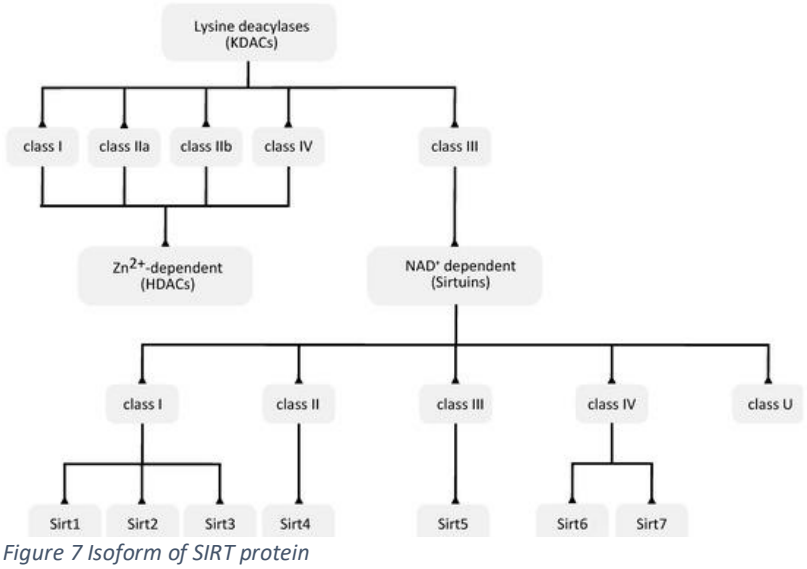

Figure 7 Isoform of SIRT protein

Figure 7: Isoforms of Sirtuin mammalian protein. (Teixeira CSS C. N., 2020)

SIRT1 is the most extensively studied homologue of sirtuin family due to its role in numerous cellular functions. Divided into 4 sub classes being Class I, II, III, IV, and U. Class I consists

of SIRT1, 2 and 3 whereas class II, III and IV comprises of SIRT4, SIRT5 and SIRT6 & 7 respectively.

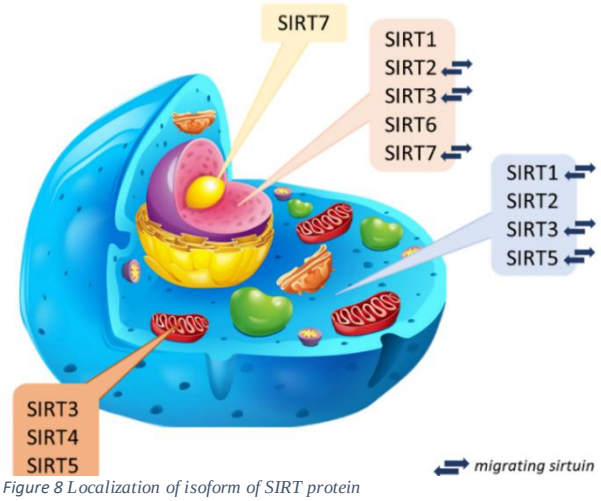

Figure 8 Localization of isoform of SIRT protein

Figure 8: Localization of different isoform of SIRT protein. (Ziętara P, 2023)

SIRT1 is present in the cell nucleus as well as can found in cytosol while dynamic cellular functions take place. Mainly found in cytosol SIRT2 has ability to translocate from cytosol to nucleus during mitosis cell cycle phases G2 and M. SIRT3, 4 and 5 all have similar targeting sequences which localizes them in the mitochondria which regulates cellular metabolism. SIRT6 is localized in nucleus heterochromatic region providing genomic stability while SIRT7 is present in nucleoli which is involved in ribosome biogenesis.

SIRT1

Localized in the cell nucleus, SIRT1 is the most studied isoform of sirtuin family. Its catalytic core comprises of two major units being a smaller subdomain made of helix loop and zinc units and NAD+ binding domain consisting of Rossman fold made up of 6 parallel β sheets and 8 α helix loops. Between the open and closed states of the enzyme, there is a considerable shift in orientation of both the domains. Its catalytic depends on this dynamic interaction since it alters substrate binding and catalysis (Davenport).

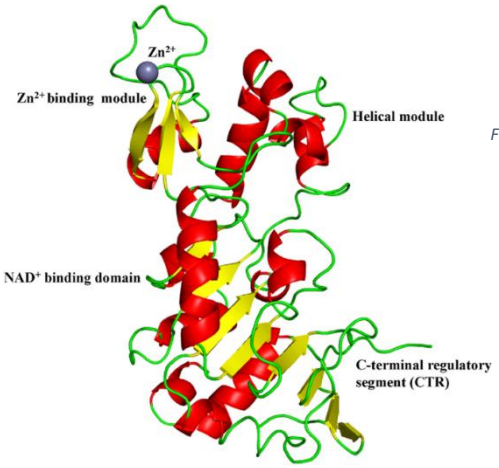

Figure 9 Molecular Structure of SIRT 1

Figure 9: Molecular structure of SIRT 1 (Sharma, 2023)

Through the deacetylation of histone residues, SIRT1, plays a crucial role in stabilizing structure of chromatin and regulating gene expression. H1 lysine 26 (H1K26ac), H3 lysine 9 (H3K9ac), and H4 lysine 16 (H4K16ac) are some of the histone targets. H4 lysine 4 (H4K4ac) was discovered to be a novel target in breast cancer samples. These are considered as its main targets since chromatin dynamics and gene transcription get affected by its acetylation activity. Acetylation of H4K16 is essential for preserving an open chromatin structure, which promotes DNA accessibility and gene expression. H3 lysine 79 (H3K79me2), defines the difference in the active and inactive chromatin domains, has higher demethylated activity due to SIRT1. SIRT1 regulates many layers of histone modifications to control chromatin state and gene expression. Research with SIRT1 KO (SIRT1−/−) highlights the vital function of the enzyme in the equilibrium of histone modifications and development. These mice show aberrant patterns of histone modification, particularly increased H3K9 acetylation and decreased H3K9me3, which are linked to embryonic mortality. This suggests that SIRT1 plays a critical role in preserving the proper ratio of histone alterations required for healthy development. Moreover, its deregulation has been linked to several malignancies (Zhang T, 2010) (Iside C, 2020).

SIRT1 overexpression has been reported in colon carcinomas, prostate cancer, and melanoma skin cancers, and leukaemia. On the other hand, liver cell carcinomas and breast cancer had lower SIRT1 levels. SIRT1's complex role in carcinogenesis is highlighted by its variable expression in malignancies, where its role switches as a tumour suppressor or oncogene. SIRT1's subcellular location affects its functionality. Its function in the nucleus has already been discussed. It plays a role in metabolism and stress response in the cytoplasm (Yuan Y, 2016) (Kwon HS, 2008).

SIRT1 role in DNA Damage Response

In DDR it targets non-histone proteins as well as histones. SIRT1 can modify chromatin structure and protein activity through dual targeting, which in turn affects cells response to damage. SIRT1 also deacetylates non-histone proteins, changing their function and assisting in DDR processes as well as cellular defense against DNA damage. The chromatin compaction function by SIRT1 is essential for DNA damage sensitivity and repair. It keeps tightly condensed heterochromatin in human fibroblasts, which prevents UV-induced photoproduct formation like CPD and 6-4PP. These photoproducts are mainly found in euchromatin because of its more open structure. Moreover, with studies on rats fed a ketogenic diet had lower levels

of oxidative stress indicators in their hippocampal regions, such as 8-OHdG, suggesting that SIRT1 has a protective function against oxidative stress. SIRT and PARP activities are enhanced by elevated NAD+ levels. It plays a protective role in the homeostasis of cellular microenvironment by indirectly shielding DNA from various forms of damage while preserving chromatin integrity. Sir proteins, which are sirtuin orthologs, polymerize across nucleosomes in yeast to form inactive heterochromatin. They then go to DNA damage sites and facilitate repair by means of ATM homolog signaling. In humans, genotoxic stress responses shift from transcriptionally suppressed loci to DNA breakage. This translocation is essential for beginning aging-related transcriptional alterations, impacting chromatin structure, and encouraging repair through ATM signaling. The spatial and temporal regulation of DNA repair, which is essential for preserving genomic integrity, is highlighted by these mechanisms and is attributed to SIRT1 (Alves-Fernandes, 2019) (Chung, 2010).

It targets DSB sites for the recruitment of repair proteins, which SIRT1 deacetylates to alter their activity. Research has demonstrated that mutant SIRT1 mouse embryonic fibroblasts (MEFs) are more susceptible to UV and γ-irradiation. This emphasizes its role in controlling the generation of γH2AX, Rad51, BRCA1, and NBS1 foci after DNA damage, which is crucial for efficient DNA repair and cell cycle checkpoints. SIRT1 deacetylates key repair proteins, such as KU70 and FOXO family members, to activate them following the damage. Along with KU80, KU70 is a component of NHEJ repair mechanism described previously that joins to broken DNA strands. Lack of KU70/KU80 reduces cell susceptibility to radiation by hindering DSB repair (Chen, et al., 2021).

Additionally, KU70 and SIRT1 interact competitively with LSD1 (lysine-specific demethylase 1). Enhanced SIRT1-KU70 association promotes chromatin opening, which aids in DNA repair and results in resistance to tyrosine kinase inhibitors and BCR-ABL mutations in chronic myeloid leukaemia (CML). Additionally, via controlling SIRT1 activity through the dephosphorylating enzyme SHP-1, KU70 influences the effectiveness of DNA repair in adult T-cell leukaemia-lymphoma (ATL) cells and, when suppressed in Jurkat-xenografted mice, reduces carcinogenesis. Transcription factor FoxO1 is a master regulator for DNA repair under stress, and is modulated by SIRT1. When pancreatic β-cells are under stress from nitric oxide, there is more DNA damage when SIRT1 is not working. FoxO1 is known to have SIRT1-dependent action. When FoxO1 is deacetylated, it translocates to the nucleus and activates transcription of repair genes like GADD45α (Ozawa, 2010).

Via the deacetylation of FoxO proteins, SIRT1 promotes the production of genes that repair DNA and inhibit apoptosis. A complex involving SIRT1 and FOXO family proteins (FOXO3 and FOXO4) prevents FoxO-induced apoptosis while simultaneously inducing cell cycle arrest and tolerance to oxidative stress. The involvement of FoxO proteins, which function as tumor suppressors, in chromosomal translocations in carcinomas highlights the essential role of SIRT1 in regulating genomic stability (Motta MC, 2004) (Yang Y, 2005)

As mentioned previously ATM and SIRT1 have a dependent relationship. In an ATM-dependent path, SIRT1 is drawn to DNA breaks where it deacetylates and activates ATM via promoting auto-phosphorylation, thereby stabilizing it at DSB sites. To ensure appropriate DNA repair, senescence, or cell death responses, ATM and ATR work cooperatively with other kinases and mediator proteins to phosphorylate a wide variety of substrates. In response to ionizing radiation, SIRT1 deacetylates NBS1, enabling ATM to phosphorylate it at Ser343. This promotes the activation of cell cycle checkpoints and the DNA repair signaling pathway. The MRN complex, which includes NBS1, MRE11, and RAD50, is essential for identifying and reacting to DNA damage. Furthermore, by deacetylating the Werner syndrome protein (WRN), SIRT1 improves the protein's interaction with several DNA repair proteins, including PARP-1, RAD52, Ku complex, MRN complex, and p53, enabling a strong response to DNA damage (Chen A. C., 2020). Moreover, SIRT1 deacetylates KAP1, stabilizing its association with 53BP1 to support NHEJ repair and obstructing repair pathways for HR. Additionally, by deacetylating XPA, SIRT1 improves NER, which is essential for repairing UV-induced DNA damage. After oxidative stress, SIRT1 also controls several DNA repair enzymes in the MMR and BER pathways. In human embryonic stem cells, SIRT1 regulates proteins such as MHS2, MSH6, and apurinic/apyrimidinic endonuclease APEX1 to preserve genomic integrity and fidelity (Lee, 2012).

Chapter 2: Materials and Methods

2.1. Buffers and Solutions

Composition of the various standard buffers and solutions prepared and used during the protocols is given below.

2.1.1. Running Buffer for SDS-PAGE

1xTris-Glycine-SDS buffer with composition 0.25M Tris-HCl (pH 8.3), 1.92M Glycine, 1% (w/v) SDS was used as running buffer for SDS-PAGE.

2.1.2. Transfer Buffer for Western Blotting

Tris-glycine buffer with composition of 25 mM Tris-HCl (pH 7.6), 192 mM glycine, and 20% methanol.

2.1.3. Tris-buffered saline with 0.1% Tween 20 (TBST)

Composition – 20mM Tris base, 150mM NaCl and 0.1% (w/v) Tween 20 detergent.

2.1.4. Buffer for DNA dilution

1xTris-EDTA buffer - 1 mM EDTA, 10 mM Tris base, pH 8.0

2.2.Primary Cell Culture

Normal human epidermal keratinocytes (NHEK) were derived from neonatal foreskin or NL and L biopsies following standard procedures.

Sample Processing

Day 1

Placed the sample on petri dish, facing the epidermis part on upside. Then removed the excess adipose tissue and then chopped the biopsy into small pieces using sterile blade. After that collected all the samples in 15 ml falcon. Gave 1 wash with HBSS+10% Anti-Anti, followed by 3 washes with 70% EtOH and then again washed with HBSS10 and anti-anti. Then added

freshly prepared and sterile filtered 0.25% dispase and incubated at 4°C for overnight in CO_2 incubator.

Day 2

Took out the falcon and dispensed all the samples in petri dish. Separated the epidermis from dermis with help of sterile blade and kept aside the separated epidermis. Chopped the dermis and added freshly prepared collagenase (1mg/ml) in it and incubated at 37°C overnight until single cell suspension is formed. Meanwhile finely minced the epidermis and transferred it into new vial and added trypsin to it and placed it in incubator at 37°C for 10-12 minutes. After that added DTI (inhibitor) to it and centrifuged it. Remove supernatant and gave 1 wash with HBSS+10% Anti-Anti. Added 2 ml M254 media in the pellet and made two T-25flask. Took 1 ml of cell suspension and added it in one flask and then added 2 ml of KSFM media and 2 ml of M254 media in it. In the second flask added 1 ml cell suspension and added 3 ml M254 media. Kept both the flask in CO_2 incubator for 48 hours.

Day 3

Checked for the single cell suspension of the dermis, when single cell suspension is formed, added media to quench and then centrifuged it. Removed supernatant and gave 1 wash with media, again remove supernatant and added DMEM+20% FBS. Added the cell suspension in T-25 flask. Kept it in CO_2 incubator for cell growth and checked after 48 hours. Henceforth, an informed consent was taken from all the patients before extracting the samples and proceeding with research studies.

2.3.Protein estimation using BCA Protein Assay

The quantification of the purified protein was done by using a kit from G-Biosciences. It was performed in a 96-well plate for as many samples as needed. The standard curve was prepared according to the ratios mentioned in the table. BSA stock of 1 mg/ml was used.

Table 1 preparation of Standard BSA mixture of BCA method

Sample No.	BSA Volume (µl)	MQ Volume (µl)	Concentration
Blank	0	25	0
1	1	24	0.0133
2	2	23	0.0267
3	4	21	0.0532
4	8	17	0.1064
5	10	15	0.1333
6	20	5	0.2667

In order to minimize error, duplicates were prepared of each sample. Volume up to 25 µl of our protein sample was added in a separate well and the final volume was made to 25 µl by adding MQ. Once all these samples were prepared, 50 parts of BCA Solution were combined with 1 part of Copper Solution (both provided in the kit) for a single well, to obtain a clear green coloured Working Solution (WS). The total amount of the WS required was calculated according to the ratio mentioned above. 50 µl of WS was added to each well and mixed properly by pipette. The plate was covered with aluminium foil and incubated at 37°C for 30 minutes. Absorbance was then taken at 562nm using a Plate Reader (TECAN). The average of each duplicate was taken to obtain a single reading for a particular sample, from this reading the average of the blank sample reading was subtracted and a standard curve was plotted keeping the concentration on the x-axis and the absorbance on the y-axis. The equation of the line of the standard curve thus obtained was used to calculate the concentration of our protein sample. It was then divided by the dilution factor in order to obtain the final concentration of our protein sample.

2.4.SDS-PAGE Gel Run

The glass plates and spacers of the gel casting unit were cleaned using Milli-Q water. The plates were then assembled with spacers on a stable and level surface to allow proper gel formation. The resolving gel solution was prepared based on the desired percentage of gel,

following the specified volumes for each component mentioned in the table below. The components were added in the specified order, with gloves worn throughout the process to ensure safe handling of acrylamide.

COMPONENTS	12%	10%	8%
MQ	3.4 ml	4 ml	4.6 ml
30% Acrylamide	4 ml	3.3 ml	2.6 ml
1.5M Tris-HCl (pH 8.8)	2.5 ml	2.5 ml	2.5 ml
10% SDS	100 µL	100 µL	100 µL
10% APS	100 µL	100 µL	100 µL
TEMED	10 µL	10 µL	10 µL

Table 2 Reaction mixture for Resolving Gel for SDS-PAGE

The prepared solution was gently mixed using a pipette and poured between the glass plates. The surface was overlaid with isopropanol to create a flat and horizontal interface. The gel was left to polymerize at room temperature for 20–30 minutes.

Once the resolving gel had polymerized, the isopropanol overlay was discarded, and the stacking gel was prepared.

STACKING GEL	
COMPONENTS	VOLUME
MQ	2.7 ml
30% Acrylamide	0.67 ml
1M Tris-HCl (pH 6.8)	0.5 ml
10% SDS	40 µL
10% APS	40 µL
TEMED	5 µL

Table 3 Reaction mix for Stacking Gel for SDS-PAGE

After thorough mixing, the stacking gel solution was poured over the polymerized resolving gel until it overflowed slightly. A comb was immediately inserted to create wells, ensuring no air bubbles were trapped in the gel or around the wells. The stacking gel was allowed to polymerize at room temperature for 20–30 minutes. Protein samples were prepared by adding

4 µL of 4x loading dye to 30 µL of each protein sample. The mixture was heated at 95°C for exactly 5 minutes to denature the proteins, and a short spin was given afterward to collect any condensation. Once the stacking gel had polymerized, the comb was removed, and the prepared samples were loaded into the wells. The gel was run at 110V for approximately 2 hours, or until the dye front reached the bottom of the gel. After the electrophoresis run, the gel was carefully removed from the glass plates and transferred for the western blotting.

2.5.Western Blotting

1. Preparation and Transfer Setup*:*

After SDS-PAGE, the stacking gel was removed, and the resolving gel was placed in transfer buffer. The PVDF membrane was activated by submerging it in methanol.

A sandwich-like structure was constructed in the following order:

- Sponge
- Filter pad
- Gel
- PVDF membrane
- Filter pad
- Sponge

The blot (PVDF membrane) was placed on the cathode side, and the gel was positioned on the anode side. The cassette was closed carefully, ensuring no air bubbles were trapped within the sandwich.

2. Transfer Process*:*

The cassette was placed in a transfer tank filled with transfer buffer, accompanied by an ice block to maintain low temperature. The tank was either placed in an ice bath or kept in a cold room (4–5°C) during the transfer. The transfer was conducted at 110V for 2 hours.

3. Blocking and Antibody Incubation*:*

After the transfer, the PVDF membrane was carefully removed and placed in a plastic box. It was blocked using 5% BSA prepared in TBST for 1 hour on an orbital shaker to prevent nonspecific binding.

- Primary Antibody Incubation: The membrane was incubated overnight at 4°C with the primary antibody (polyclonal TG1). Constitution of primary antibody - 1X TBST, 5%BSA, 1:1000 dilution.
- The next day, the membrane was washed three times (for 10 minutes each) with TBST

on an orbital shaker.

- Secondary Antibody Incubation: The membrane was incubated with an HRP-conjugated secondary antibody (monoclonal anti-rabbit) at room temperature for 1 hour on the orbital shaker.

4. Washing and Detection*:*

After secondary antibody incubation, the membrane was washed three times (for 10 minutes each) with TBST on an orbital shaker. Protein bands were detected using an Enhanced Chemiluminescence Reagent (ECL) and visualized using the LAS500 imaging system.

2.6. Transfection

Transfection is a process by which exogenous nucleic acids are transferred into eukaryotic cells through non-viral methods.

Cells were seeded in a suitable culture vessel, such as a 6-well plate, 24 hours prior to transfection to allow them to adhere and reach the optimal stage for transfection. On the day of transfection, the DNA was diluted in Opti-MEM in a sterile tube and mixed gently. In a separate tube, Lipofectamine reagent was also diluted in Opti-MEM and incubated for 5 minutes at room temperature. Then combined the diluted DNA solution with the diluted Lipofectamine, dropwise, mixed gently, and incubated at room temperature for 10-20 minutes to allow the formation of lipid-DNA complexes. After the incubation period, added the mixture dropwise to the cells, and the plate was gently swirled to ensure even distribution Again added 800 µl of Opti-MEM in the well to made final volume 1 ml. Incubated it for 6 hours at 37^{o}C in CO_2 incubator.

After 6 hours removed Opti-MEM media and gave 1 was with PBS and then added freshly prepared complete media. Then again incubated it for 48 hours in CO_2 incubator.

2.7.Isolation of RNA

The RNA for the epidermis layer can be directly isolated which was kept in 500 µl trizol. In addition to it, the layer is first homogenized that is mixed evenly using a homogenizer machine. Once the layer fully diminishes then proceed for isolation process but in case of dermis the process can be directly done and there is no need for homogenizing the cells. Then chloroform is added (1/5th) of the volume. After vortex, it is spined at 15 minutes, for 13000 RPM on 4

degrees Celsius. Further, three layers are extracted namely upper layer is aqueous layer (RNA), middle white layer (DNA) and pinkish layer (Protein). The aqueous layer is extracted and stored in isopropanol overnight. Following day, RNA samples are washed thrice with 70% molecular grade EtOH for 13000 RPM at 4°C. Keep it for drying for 20 minutes. After, that NFW (20µl) was added to dissolve the sample and nanodrop readings was taken.

2.7.1. cDNA Preparation from RNA

While cDNA preparation we used, iScript cDNA synthesis Kit from Bio-Rad. Reaction Mixture was prepared using iScript Reaction mix (4ul) and Reverse Transcriptase (1ul) for 1ug cDNA including NFW. So, total 5ul of reaction mix was prepared and added to the 15ul extracted RNA which was isolated earlier. The samples are added to T100 Thermal Cycler and the run is for 28 minutes. Initially the machine cycle is at 25°C for 5 minutes, secondly for 20 minutes at 46°C, then followed by 1 minute at 95°C and finally infinite hold at 105°C. Lastly, 20ul of cDNA was stored for external storage.

2.8.RT-PCR (Roche LC480 thermocycler)

After, cDNA preparation we proceeded for RT-PCR. A master mix was made including NFW + SyBR Green + cDNA with respect to the gene of interest (test gene) herein, IL4, IL-13, IL-17, IL-22 and IL-31. The cDNA is added before SyBR Green due to the viscosity as if cDNA is added afterwards then it might not mix properly. Keep vortexing and give short spin after each step. Then in the 96 well-plate the prepared master mix is added (doublets), from it 5ul is added into the 364 well plate making triplicates. Further, the 384 well plate is placed into the Roche LC480 thermocycler. In the thermocycler, the one complete cycle comprises of 95°C for 5 minutes (Preincubation stage), 60oC for 15 seconds (Amplification Stage), 95oC for 5 seconds (Melting Stage) and 40°C for 10 seconds (Cooling Stage). The whole PCR protocol is for 50 cycles.

2.8.1. RT-PCR Analysis using double – ΔΔCt method

The data analysis is done by normalizing the 18s rRNA levels. The Ct vale is taken of the required gene of interest (test gene) when we subtract the 18s value from the gene of interest. The RT-PCR data is generated in form of replicates so there should be a standard difference of 0.5 between the values as more than that it is eliminated. We use Mann-Whitney test for calculating Ct values for lesional-skin and non-lesional skin. Fold change calculation was conducted using 2 -ΔΔCt (ΔΔCt meaning ΔCt of lesional and ΔCt of non-lesional skin). We used 18s rRNA as the normalized gene to compare the fold changes expression levels for the lesional skin and non-lesional skin. If the value is more than 1.5 then the gene expression is said to be upregulated, less than 0.65 it is said to be downregulated and if anything in between it is then non-regulated

2.9.CPD Quantitation Assay

CDP-DNA standards or unidentified DNA samples are initially heat denatured prior to being adsorbed to a 96-well DNA high-binding plate. The CPDs in the sample or standard are probed with an antiCPD antibody, then with an HRP conjugated second antibody. CPD content in an unknown sample is measured by comparing against a standard curve that was derived from predetermined CPD-DNA standards.

Standard Curve –

- Incubated a solution of CPD-DNA (25 µg/mL) and Reduced DNA (200 µg/mL) at 95ºC for 10 minutes and then cooled rapidly on ice for 10 minutes to obtain single-stranded DNA.
- Diluted the denatured 25 µg/mL stock in cold TE Buffer to 4 µg/mL working concentration, whereby, for example, 8 µL is added to 42 µL of cold TE Buffer.
- Reduced DNA at 4 µg/mL is freshly prepared by diluting the denatured 200 µg/mL stock with cold TE Buffer, for example, 40 µL into 1.96 mL of cold TE Buffer.
- Prepare a set of CPD-DNA standards according to Table.

Standard Tubes	4 µg/mL Denatured CPD DNA (µL)	4 µg/mL Denatured Reduced DNA (µL)	CPD-DNA Conc. (ng/mL)
1	10	390	100
2	200 of tube #1	200	50
3	200 of tube #2	200	25
4	200 of tube #3	200	12.5
5	200 of tube #4	200	6.25
6	200 of tube #5	200	3.13
7	200 of tube #6	200	1.56
8	0	200	0

Table 4 Preparation of standard CPD-DNA solution for CPD quantitation assay

Assay Procedure –

- Isolated DNA from cell or tissue samples with a commercial DNA Extraction kit.
- Denatured DNA sample to single-stranded DNA by incubating the sample at 95ºC for 10 minutes and quickly chilling on ice for 10 minutes.
- Diluted DNA samples to 4 µg/mL in cold TE Buffer.
- Added 50 µL of unknown DNA samples or CPD-DNA standards into the wells of the DNA High Binding plate.
- Added 50 µL of DNA Binding Solution to each well. Pipet well to mix and incubate overnight at room temperature on an orbital shaker. All DNA samples including standard and unknown should be assayed in duplicate.
- Discarded the DNA solutions and wash twice with PBS. Removed excess fluid. Added 200 µL of Assay Diluent to every well and block for 1 hour at room temperature.
- Discarded the Assay Diluent. Added 100 µL of diluted Anti-CPD Antibody to all wells and incubated for 1 hour at room temperature on an orbital shaker.
- Washed 5 times with 250 µL of 1X Wash Buffer with aspiration between each wash. Followed the final wash, discarded wells and tap microwell strips on absorbent pad.
- Added 100 µL of the diluted Secondary Antibody-HRP Conjugate to all wells and incubated for 1 hour at room temperature using an orbital shaker. Washed the wells in strip wells 5 times.
- Brought Warm Substrate Solution to room temperature. Dispensed 100 µL of substrate solution in each well, including blanks. Incubate room temperature using an orbital shaker.
- Stopped enzyme reaction by adding 100 µL of Stop Solution to every well.
- Read absorbance of every well using a microplate reader with 450 nm as main wave length. Employ the Reduced DNA Standard as an absorbance blank.

2.10. Immunocytochemistry (ICC)

2.10.1. Culture

Following termination of transfection, trypsinised the cells and plated the 60000 cells on sterile glass coverslips in each well. Following 36 hours of plating, initiated the ICC staining.

2.10.2. Fixation

Removed the culture medium from the dish or took out each coverslip as necessary with tweezers, and washed gently with PBS at room temperature.

Incubated coverslips in newly prepared 4% paraformaldehyde - PBS, room temperature, for 15 minutes. Or the cells could be fixed for 10 minutes in -20°C methanol.

Washed coverslips of fixative in PBS, 5 minutes.

2.10.3. Permeabilization

Incubated the coverslips with 0.5% Triton X-100 in PBS at room temperature for 5 minutes. Use the last working concentration of alternative detergents (e.g., digitonin, Tween 20) to determine what are the optimum conditions to obtain maximum preservation of cell structure and protein of interest.

Washed coverslips of the permeabilization buffer by incubation with PBS for 5 minutes.

2.10.4. Bloking

For background fluorescence reduction, blocked the coverslips with 1-5% normal serum or BSA in PBS at room temperature for 1 hour.

2.10.5. Antibody Incubation (ICC STAINING)

Solved primary antibody dilutions for ICC in 1% normal serum or BSA. Common working concentrations of antibodies can be between 5-20 µg/ml, but each antibody might need to be optimized for the right signal to be achieved.

Incubated the coverslips in the primary antibody dilution for 1 hour at room temperature (37°C is optional) or overnight at 4°C.

Gently washed the coverslips three times for 5 minutes each in PBS. Further or extended washes may be necessary if there is still too much background.

Prepared a suitable dilution of secondary antibody conjugated with fluorochrome in 1% normal serum or BSA. Standard initial dilutions are 1-2 µg/µL, but optimization can be needed for optimal image.
Incubated the coverslips for 1 hour at room temperature in a dark place in the secondary antibody dilution.

Washed the coverslips carefully in PBS three times 5 minutes each. More or longer washes could be necessary if too much background persists.

2.10.6. Mounting and Imaging

Once all washing steps have been done, the coverslips may be counter stained with DAPI or Hoechst (1-10 µg/mL) in order to stain the nuclei.

Placed the coverslip inverted onto a glass slip and added a drop of mounting media that includes a fluorescence antifade agent.

Removed the excess mounting media carefully if needed and sealed accordingly with transparent nail polish.

Placed the cells under a fluorescence microscope and imaged as needed.

Chapter 3: Results and Discussion

3.1 The lesional epidermis of vitiligo exhibits dysregulated expression of SCF

The SCF-cKIT pathway is involved in the survival and proliferation of epidermal melanocytes. Its regulation, however, is ambiguous in vitiligo with some research proving its upregulation while others prove SCF to be downregulated (Lee, Kim et al. 2005, Moretti, Fabbri et al. 2009). Therefore, we chose to quantify the transcript levels of SCF-a (membrane-associated), SCF-b (soluble variant) in patients with stable, non-segmental vitiligo by RT-PCR and identified them to be invariably upregulated in L compared to NL epidermis (SCF-a $p<0.0017$, $n=6$; SCF-b $p<0.0003$, $n=7$; Figure 10a). SCF was substantially increased in L compared to NL epidermal lysates at protein level too (Figure 10b, c). In addition, cKIT, the SCF receptor, was also upregulated at mRNA levels ($p<0.047$, $n=4$, Figure 10d) Increased levels of SCF and cKIT in the absence of melanocytes, their usual recipients, led us to speculate that SCF was likely acting on keratinocytes itself, autocrinally. As SCF-a (the membrane-bound type) is known to exert its action on melanocytes and remaining attached to the keratinocyte-plasma membrane, we chose to use the soluble form of SCF (recombinant human SCF-b) to mimic the physiology of SCF in keratinocytes.

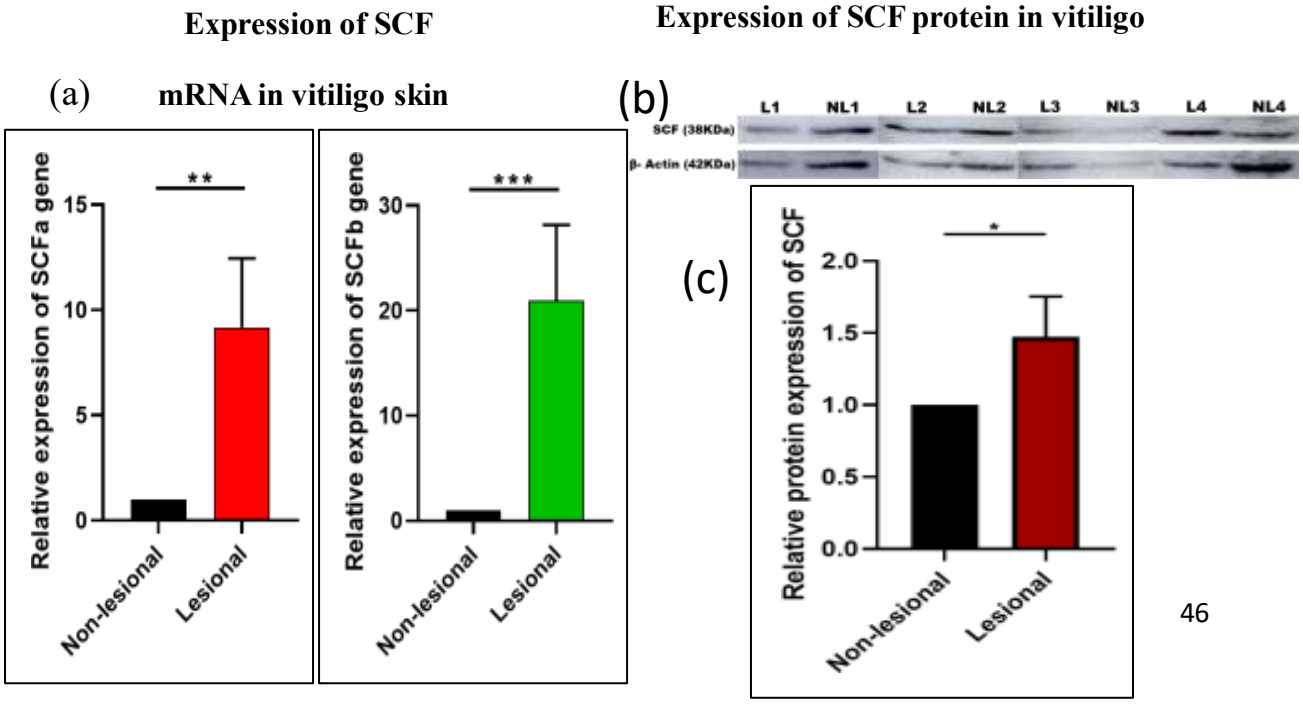

(d) Expression of cKIT receptor

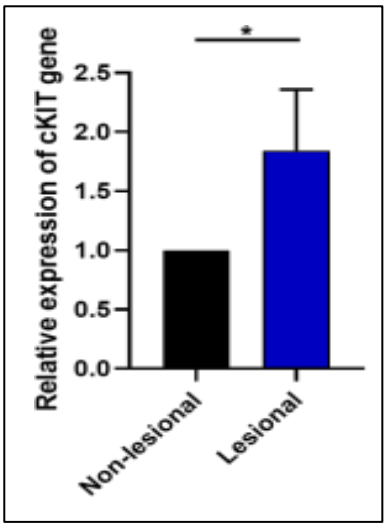

Figure 10 Expression of SCF and cKIT at transcriptional level

Figure 10. Exogenous SCF causes a unique transcriptional response in primary keratinocytes: Plotting the fold change with respect to the NL epidermis shows the transcriptional regulation of (a) membrane-bound SCF-a (n=7) and soluble SCF-b (n=6), (b) SCF levels at protein levels in epidermal lysates (n=4), (c) and its quantification (d) cKIT receptor (n=4) in NL and L epidermis (n=3).

3.2 Keratinocytes induce a distinct transcriptional response when treated with exogenous SCF

In the absence of its traditional recipient melanocytes, an overexpression of SCF in L skin prompted us to consider the possibility that SCF might contribute to keratinocyte biology. To determine whether or not keratinocytes were responsive to SCF, we cultured NHEK with previously applied concentrations of rhSCF intended to drive melanogenesis (Yun, Roh et al. 2020). Normal human epidermal melanocytes (NHEM) exposed to the same concentrations of rhSCF were controls. A genome-wide transcriptome study followed by Gene Set Enrichment Analysis demonstrated a unique subset of genes/processes to be highly upregulated in SCF-treated-keratinocytes compared to melanocytes (supplementary figure 1a). Although the introduction of SCF caused upregulation of the melanogenesis pathway in melanocytes (supplementary figure 1b); calcium signalling, chemokine, cell adhesion and cytokine-cytokine signalling pathways were exclusively found to be upregulated in SCF-treated keratinocytes

(supplementary figure 1b), indicating the capability of keratinocytes to respond to SCF in a way different from the melanocytes. Since SCF at both concentrations elicited similar response in keratinocytes, we selected lower concentration (50ng/ml) for further use.

3.3SCF signaling provides protection to keratinocytes against UV-B induced DNA damage

Because the most ubiquitous physiological stress tolerated by the skin is exposure to UV radiation, we speculated that SCF may be mediating protection against UV-mediated cellular injury. To examine whether SCF afforded any protective benefit to keratinocytes against UV-B irradiation, additional experiments were conducted using normal human epidermal keratinocytes (NHEK), i.e., primary keratinocytes. SCF-treated NHEK were exposed to 10mJ/cm2 UV-B and DNA damage assessed. There was a considerable decrease in γ-H2AX positivity and cyclobutane pyrimidine dimers (indications of UV-B induced DNA damage) in SCF-treated cells compared to control cells, which indicates the protective effect of SCF against UV-B induced DNA damage (Figure 11 a-c). To find out if SCF had its effects mediated through binding with the cKIT receptor, NHEK cells were treated with SCF under conditions of with or without imatinib, a cKIT inhibitor. Imatinib treatment resulted in reversal of the reduced γ-H2AX positivity (Figure 11 a, b) and CPD formation (Figure 11c) observed with SCF addition in NHEK, validating SCF to indeed be acting via the cKIT receptor. SCF under conditions of with or without imatinib, a cKIT inhibitor Imatinib treatment resulted in reversal of the reduced γ-H2AX positivity (Figure 11 a, b) and CPD formation (Figure 11c) observed with SCF addition in NHEK, validating SCF to indeed be acting via the cKIT receptor.

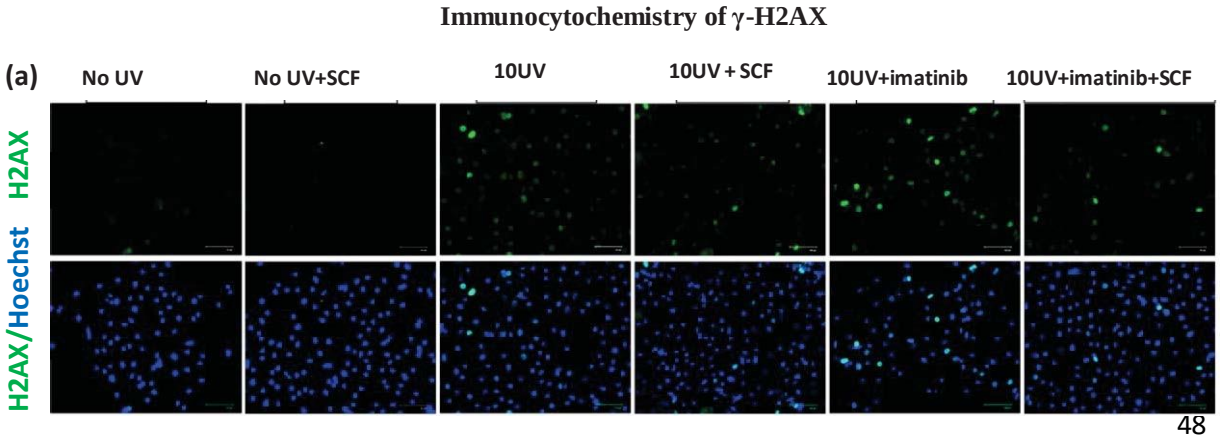

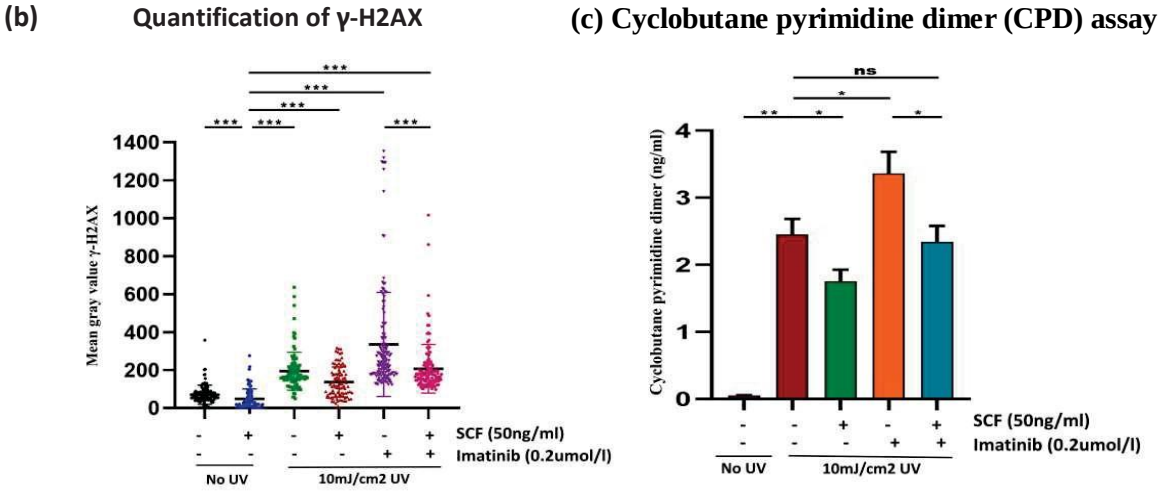

Figure 11 Reduced DNA damage upon SCF treatment

Figure 11. SCF signaling decreases UVB-induced DNA damage in keratinocytes: Intensity of γ-H2AX staining (green) in HaCaT cells treated with SCF in absence or presence of 10mJ/cm2 of UV-B radiation. Intensity of γ-H2AX staining (green) after treatment with Imatinib (inhibitor for cKIT), or SCF+ Imatinib in UV-B treated cells is also shown. Scale bar is 10 microns. (b) Scatter plot of mean grey values (γ-H2AX intensity corrected with background) in cells for treatments shown in 11(a). Every point on the plot is a single cell. Standard error of mean is represented by horizontal line. (c) CPD formation after treatment with SCF and/or imatinib in UV-B irradiated cells plotted as bar graph (n=3). *p<0.05, **p<0.01, ***p<0.001.

3.4 SCF reduces UV-B induced mitochondrial fission and enhances mitochondrial bioenergetics

In addition to DNA damage, UV-B irradiation induces mitochondrial fragmentation and ROS production (Larsson, Andersson et al. 2005, Wang, Wang et al. 2015). Therefore, we examined the impact of SCF on UV-B-induced mitochondrial impairment and observed mitochondrial ROS to be considerably reduced in NHEK cells treated with SCF compared with controls (Figure 12 a). SCF was also seen to rescue the NHEK cells from UV B triggered lipid peroxidation (Supplementary Fig S2). Measurement of mitochondrial health

demonstrated SCF-treated, UV-B irradiated cells to have longer (healthier) mitochondria i.e., higher aspect ratio and lower circularity, than UV-B treated controls (Figure 12 b, c). Because mitochondrial fission and fusion primarily rely on the delicate equilibrium between proteins such as dynamin-related protein 1 (DRP1, promotes fission) and mitofusin 1 (MFN1, promotes fusion) (Hoppins, Lackner et al. 2007, Zemirli, Morel et al. 2018), their expression levels were tested with western blot. Whereas UV-B irradiation resulted in a large induction of the levels of DRP1, SCF treatment resulted in its large downregulation, as seen microscopically with the elongated mitochondria (mitochondrial fusion) (Figure 12 d, e). The expression of MFN1 was found to be significantly upregulated in SCF-treated cells as compared to controls. Next, other mitochondrial fission (FIS1) and fusion gene regulation was found at the mRNA level. While the expression of OPA1 was found to be significantly upregulated in SCF-treated cells, FIS1 was significantly downregulated as compared to controls (Supplementary Fig S3). To explore mitochondrial morphology in greater depth, ultrastructural analyses (TEM) were used that indicated the existence of a much higher proportion of healthy mitochondria (well-developed cristae) in SCF-treated cells compared to controls that were made up largely of harmed mitochondria (degenerated cristae) (Figure 12f, g). Lastly, we measured the rate of oxygen consumption by keratinocytes and observed SCF to enhance basal respiration and ATP output in UV-B irradiated cells (measured following oligomycin treatment, a complex V inhibitor; Fig 12 h, i). But the spare respiratory capacity (determined after adding Carbonyl cyanide-4 (trifluoromethoxy) phenylhydrazone or FCCP, an uncoupler) and non-mitochondrial respiration (determined after the addition of complex I and III inhibitors-rotenone and antimycin A respectively) was similar in SCF-treated cells and controls (UV-B treated cells) (Supplementary Fig S4).

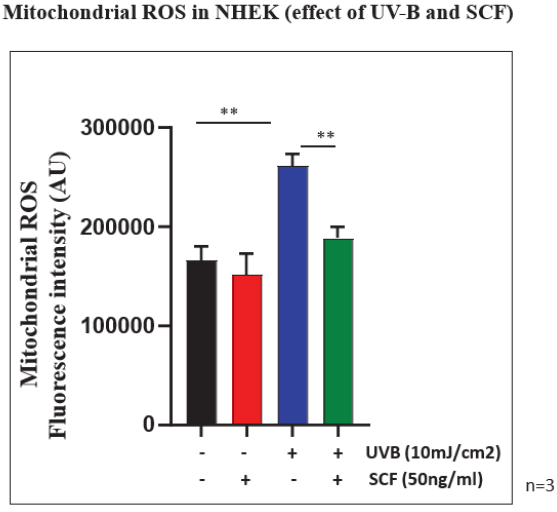

(b) Mitochondrial shape determination (Confocal)

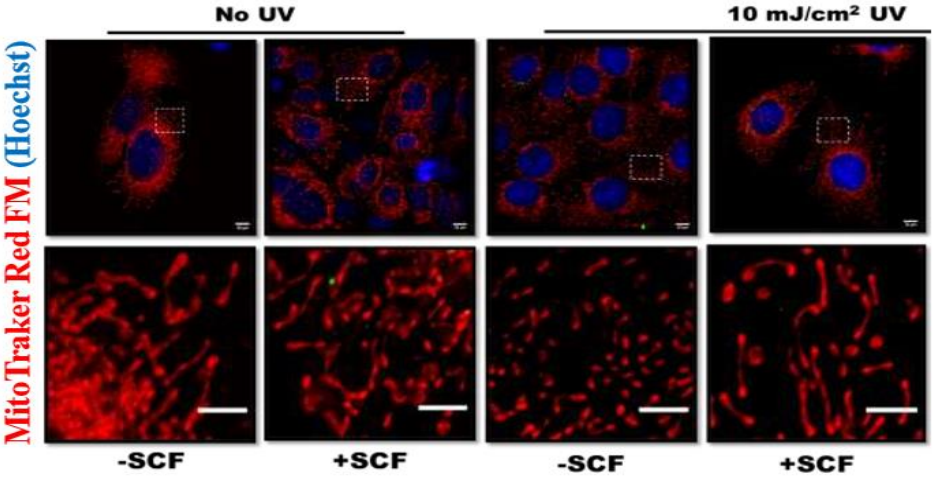

(c) Quantification of mitochondria (confocal)

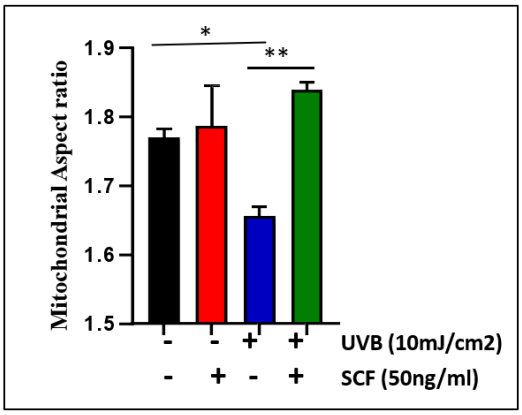

(d) Immunoblot of MFN1

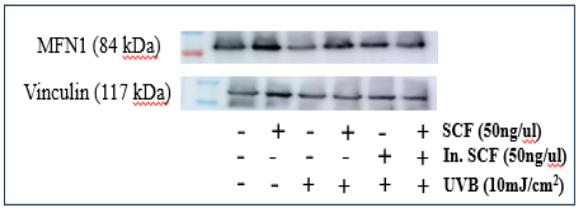

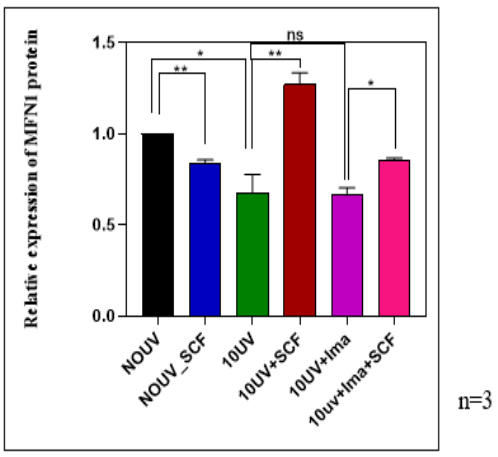

(e) Immunoblot of DRP1

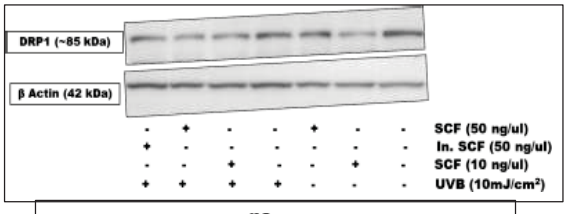

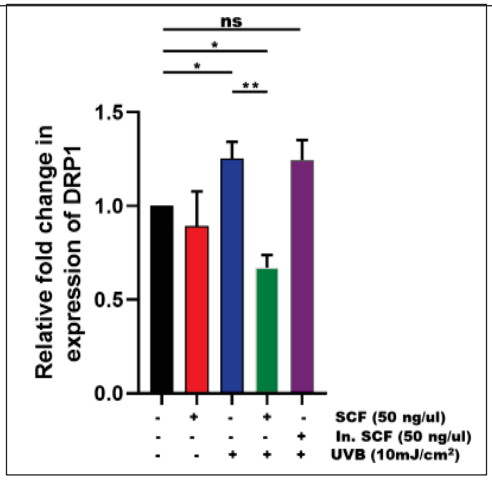

(g) Mitochondria (TEM)

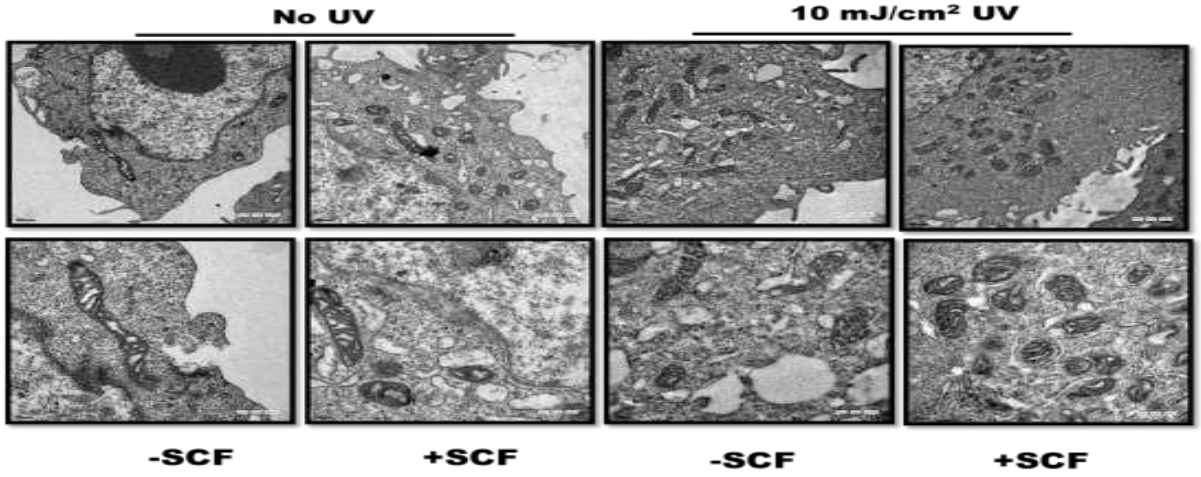

(h) Quantification of mitochondria (TEM)

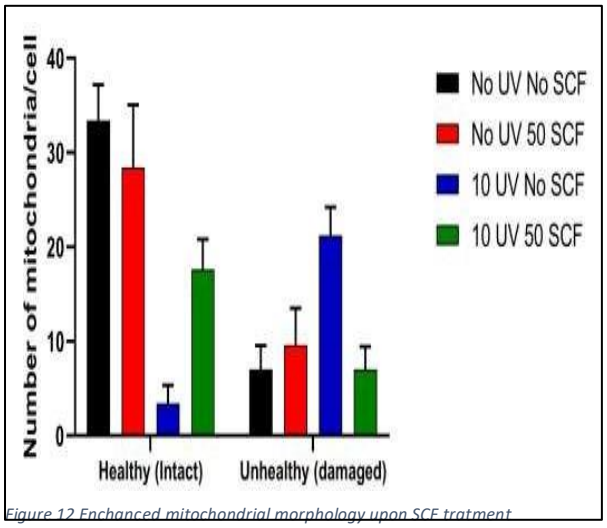

(i) Quantitation of Mitochondrial bioenergetics

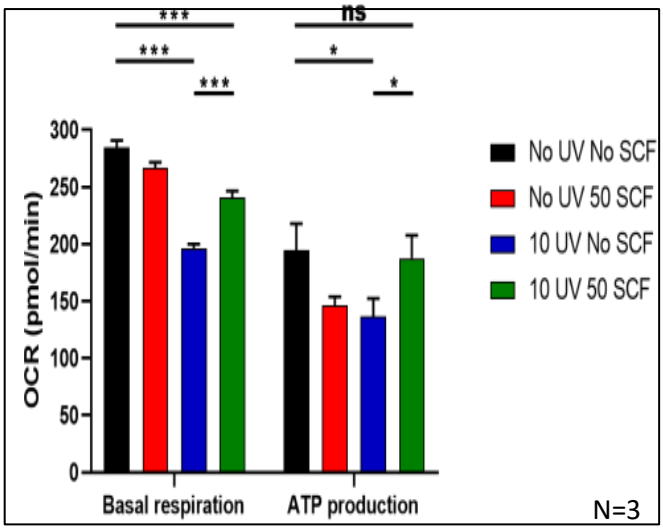

Figure 12. SCF regulates mitochondrial morphology:

(a) Bar graph indicating fluctuations in ROS in cells following SCF treatment with or without 10mJ/cm2 of UV-B irradiation (n=3). ROS was quantitated in arbitrary units. (b) Overviews and enlargements (bottom panel) of mitochondria seen by MitoTracker Red FM staining after treatment with SCF with or without UV-B (confocal microscopic images) and (c) its quantitation (aspect ratio) with Image J analysis. (d) Western blot analysis of MFN1 protein and its densitometry and (e) western blot analysis for mitochondrial fission protein DRP1 and its densitometry from ImageJ software (n=3, *P<0.05, **P<0.01, ***P<0.001). Beta-actin and vinculin was normalized as a control (f) Representative TEM images and magnified areas (lower panel) illustrating mitochondrial morphology of keratinocyte cells treated with SCF in presence or absence of UV-B. Black arrows indicate healthy mitochondria and red arrows indicate degenerated mitochondria (g) Quantitation of the TEM images (n=10 cells, 2 independent experiments) to determine mitochondrial health on the basis of their morphology

(cristae) (h) Graphs of mitochondrial bioenergetics of cells measured on seahorse XFe24 OCR analyser and (i) quantitation of basal respiration and ATP production on SCF treatment in presence or absence of UV-B (n=3) *p<0.05, **p<0.01 ***p<0.001.

3.5SCF modulates lipid metabolism in keratinocytes exposed to UV-B radiation

Ultrastructural examination, carried out to assess mitochondrial health, surprisingly showed a physical close association of mitochondria with lipid droplets, the cellular lipid stores (Supplementary Fig S5). To see how UV-irradiation was controlling lipid droplets in keratinocytes, NHEK cells were Bodipy-stained, a selective stain for neutral lipids. Confocal imaging of Bodipy-stained NHEK demonstrated a higher concentration of lipid droplets in UV-B irradiated compared to unexposed cells (Figure 13 a, b). Additionally, inclusion of SCF was found to decrease the lipid droplet population significantly in UV-B exposed NHEK cells (Figure 13 a, b). In contrast, lipid droplet size in UV-B exposed cells did not differ significantly from unexposed cells (Supplementary Fig S6). Likewise, a remarkable decrease in TAG levels in UV-B irradiated whole cell lysates of NHEK indicated towards the capability of SCF in reversing the increase in TAG levels caused by UV-B (Figure 13 c). A remarkable decrease in the accumulation of lipid droplets and TAG content led us to study the control of lipoprotein lipase (LPL), a limiting enzyme in the formation and storage of lipid droplets (Loving, Tang et al. 2021) and hydrolysis of TAG-lipoproteins (Wang and Eckel 2009). In fact, LPL was significantly upregulated at the transcript level in SCF-treated NHEK cells after UVB-exposure (p<0.01, Fig 4d). Clinical sample analysis also showed a significant upregulation of LPL in L compared to NL epidermis (p<0.04, n=4, Supplementary Figure S7)

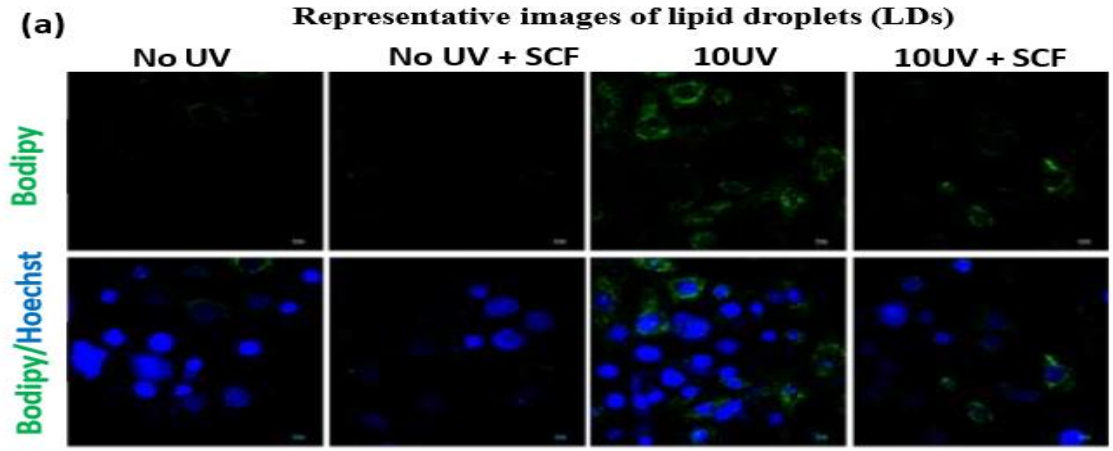

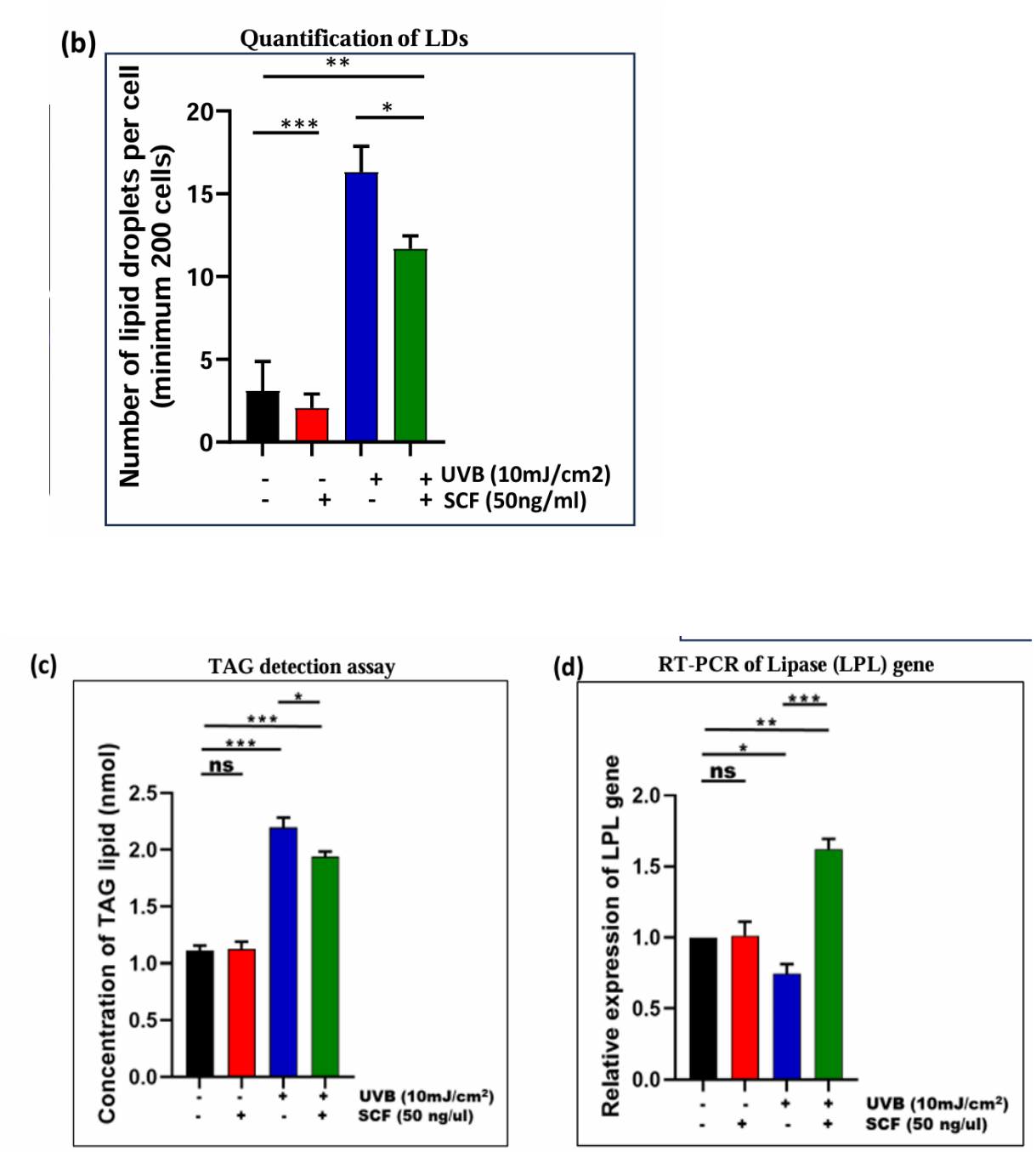

Figure 13 SCF regulates lipid formation and metabolism

Figure 13: SCF controls UV-B mediated lipid droplet formation and lipid metabolism- (a) Representative pictures and (b) quantitation (count) of lipid droplets as seen by Bodipy staining in NHEK treated with or without UV-B with or without SCF under confocal microscope (n=3). (c) bar graph depicting TAG levels as assayed by lipase-based estimation in NHEK treated with or without UV-B with or without SCF (n=3). (d) bar graph showing transcriptional expression of LPL in NHEK treated with or without UV-B in presence/absence of SCF (n=3). *p<0.05, **p<0.01, ***p<0.001

3.6 SCF-induced reprogramming of lipid metabolism provides protection to keratinocytes against UV-B induced DNA damage

As the addition of SCF had a considerable decrease in both the formation of lipid droplets as well as DNA damage in UV-B irradiated cells, we aimed to determine if the modulation of lipid droplets had any influence on UV-B induced DNA damage in keratinocytes. Orlistat treatment of NHEK, a noted lipase inhibitor (Heck, Yanovski et al. 2000), which indeed caused a rise in lipid droplet accumulation (Figure 5a, b), also coincided with a dramatic rise in UV-B induced DNA damage as reflected by an increase in γ-H2AX positivity (Figure 14 c, Supplementary Fig S8) and CPD formation (Supplementary Fig S10). In contrast, NHEK treatment with a known agonist of LPL, NO-1886 (Tsutsumi, Inoue et al. 1993), resulted in a dramatic decrease in UV-B induced DNA damage as indicated by γ-H2AX positivity and CPD formation (Figure 14 c, Supplementary Fig S8, 9) accompanied by decreased lipid droplet accumulation in the cells (Figure 14 a, b). In addition, co-treatment of SCF in orlistat-treated cells was unable to fully rescue the DNA damage and the lipid droplet accumulation compared to SCF treatment alone (Figure 14 a, b, c) indicating a pivotal role of lipid metabolism in SCF-mediated protective response in UV-irradiated keratinocytes. To further investigate the role of LPL in regulating lipid metabolism in UV-irradiated cells, we knocked down its levels by a siRNA-based approach. A heightened DNA damage (γ-H2AX positivity) and the number of lipid droplets following siLPL treatment (Figure 14 d-f) supported the findings with orlistat. As with SCF and orlistat co-treatment experiments, SCF addition to siLPL-transfected cells also couldn't fully restore the impact of LPL downregulation, both in lipid droplet accumulation (Figure 14 d, e) as well as DNA damage (Figure 14 f). These findings indicated that SCF provided protection against UV-B induced DNA damage by inducing lipolysis through LPL upregulation.

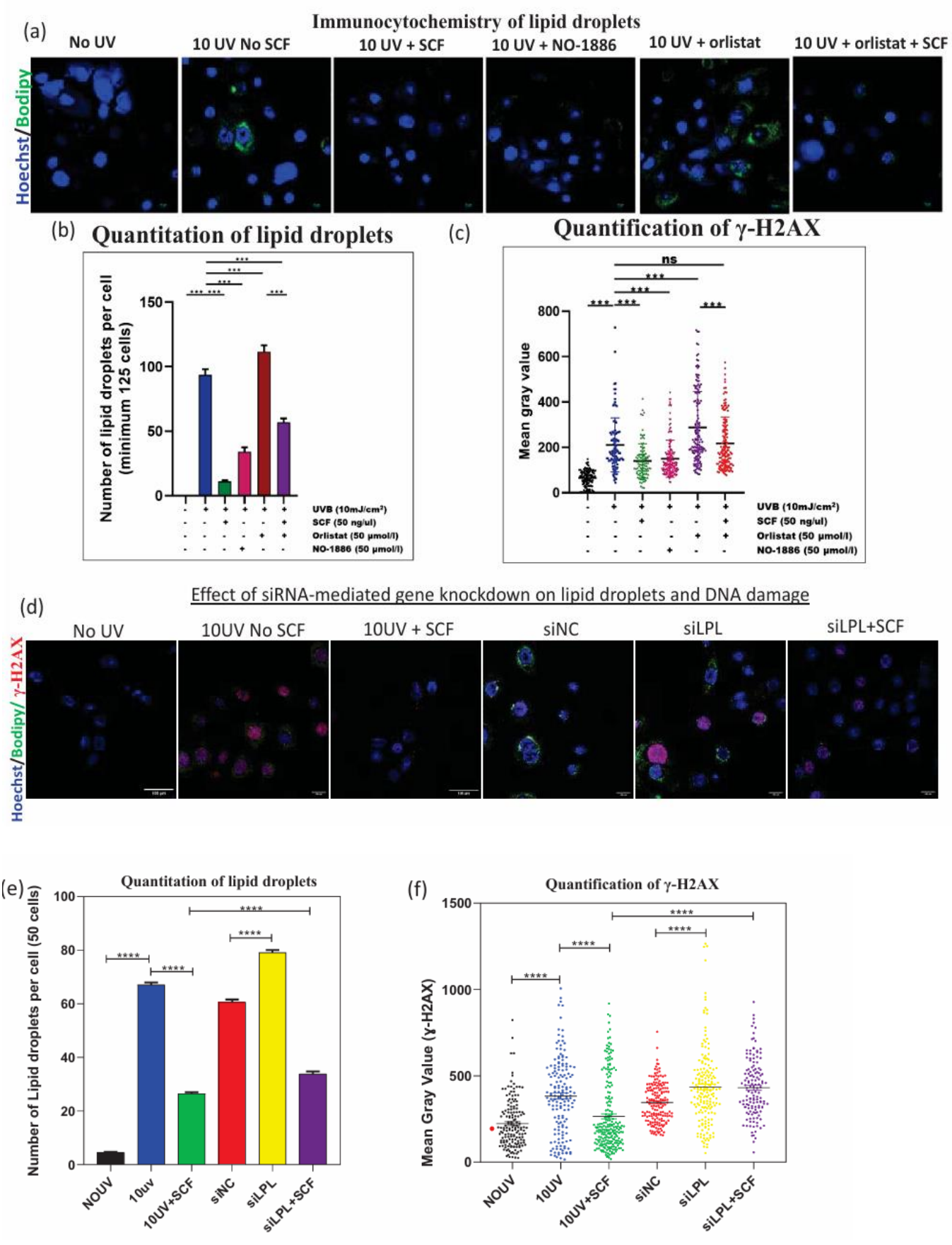

Figure 14 SCF induced reprogramming of lipid metabolism protects against UV-B induced DNA damage

Figure 14 SCF-induced reprogramming of lipid metabolism provides protection to keratinocytes against UV-B induced DNA damage

In this study, SCF-induced shift of lipid metabolism was shown to offer protection to keratinocytes, with representative images being shown in panel (a) and quantitation (in terms of numbers) of lipid droplets in NHEK treated with different combinations of SCF, NO-1886 (LPL agonist), or orlistat (lipase inhibitor) upon UV-B irradiation being shown in panel (b); visualized using a confocal microscope. Scale bar represents 10 microns. (c) Scatter plot indicating the quantification of γ-H2AX positivity in NHEK where SCF, NO-1886, and orlistat, or a combination of SCF and orlistat were used to treat UV-B-exposed cells. (d) Representative images of staining for γ-H2AX (red) and lipid droplets (Bodipy® stain, green) in NHEK after exposure to siLPL, SCF or the combination and (e) number of lipid droplets after exposure as shown in 14 (d) and (f) scatter plot representation of γ- H2AX intensity after treatments with combinations of SCF, siLPL, siLPL + SCF in UV-B irradiated NHEK using confocal microscope (n=3). *p<0.05, **p<0.01, ***p<0.001.

3.7 SCF-induced upregulation of lipoprotein lipase activates SIRT1 to defend keratinocytes against UV-B induced DNA damage

In a previous study, we had shown a significant role of SIRT1, an NAD-dependent deacetylase, in protecting keratinocytes from UV-B mediated injury (Brahmbhatt, Gupta et al. 2021). We therefore wanted to determine if the downstream consequence of SCF-LPL signaling was being mediated by SIRT1 itself. Whereas SCF treatment produced dramatic upregulation of SIRT1 protein, co-addition of SCF in orlistat-treated or in siLPL-transfected NHEK produced dramatic downregulation of SIRT1 expression (Supplementary Figure S11). Consistent with reduced accumulation of lipid droplets and DNA damage, treatment with the LPL agonist NO-1886 resulted in a significant increase in the levels of SIRT1 in NHEK (Supplementary Figure S10), implicating LPL to mediate its protective effects via upregulation of SIRT1. Subsequently, we co-treated NHEK with SCF and Ex- 527, a pharmacological SIRT1 inhibitor, that eliminated the cytoprotective effect induced by SCF through a significant elevation of lipid droplet accumulation (Figure 15 a, b) as well as DNA damage (Figure 15 c, Supplementary Fig S11, S12). In addition to treating with a pharmacological

SIRT1 inhibitor, we also used siRNA methodology to knock down SIRT1. SCF addition to siSIRT1-transfected cells also wasn't able to fully rescue the cells from the harmful action of UV-B (versus SCF treatment), both regarding lipid droplet accumulation (Figure 15 d, e) and DNA damage (Figure 15 d, f), indicating that SIRT1 upregulation was crucial for the protective action of SCF. Additionally, co-treatment of NHEK cells with siSIRT1 and NO-1886 also drastically inhibited the protective action mediated by LPL agonist NO-1886, as indicated by a drastically enhanced γ-H2AX positivity (Figure 15 d, f), indicating SIRT1 upregulation to be crucial for SCF-LPL mediated protection against UV-B induced DNA damage. In total, our findings implicated SIRT1 to be the ultimate effector protein in SCF-LPL-SIRT1 signaling axis.

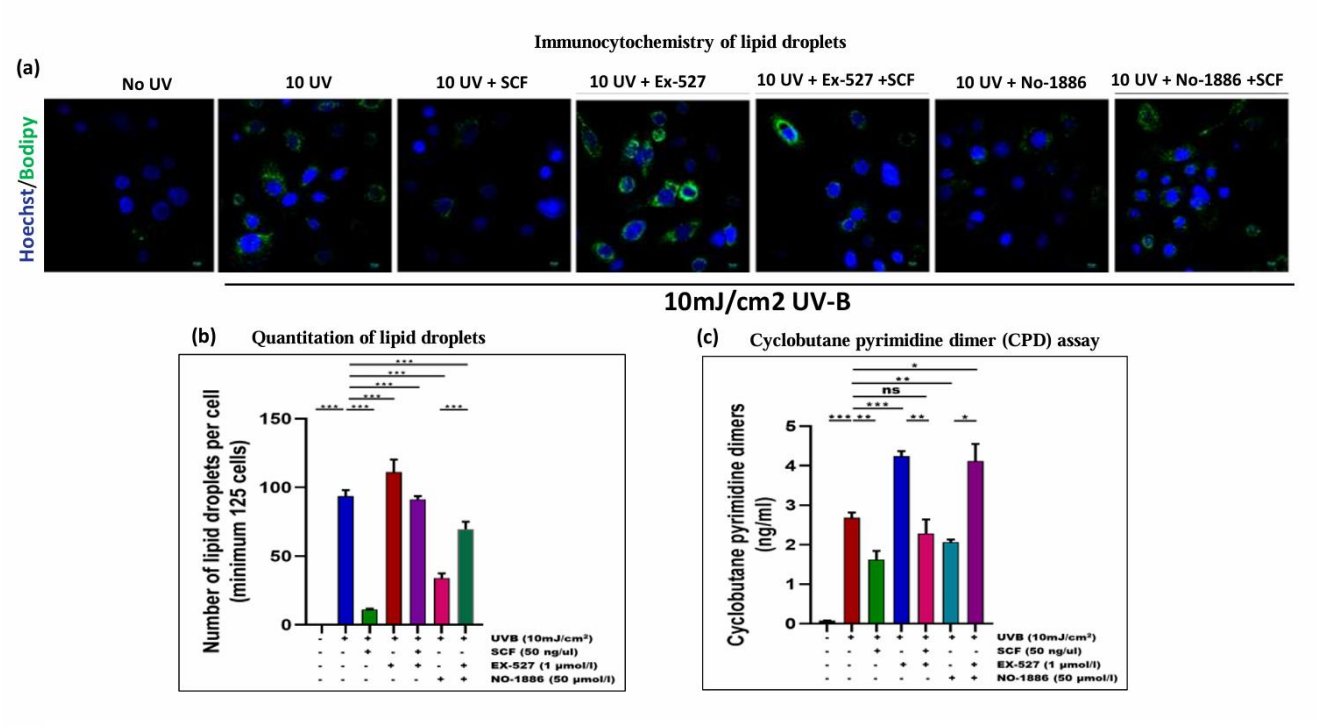

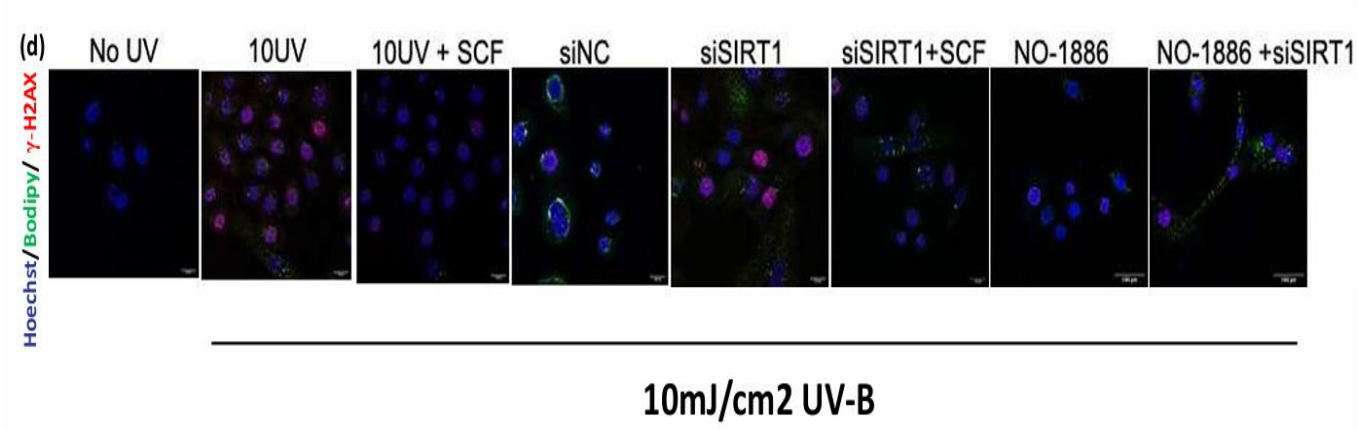

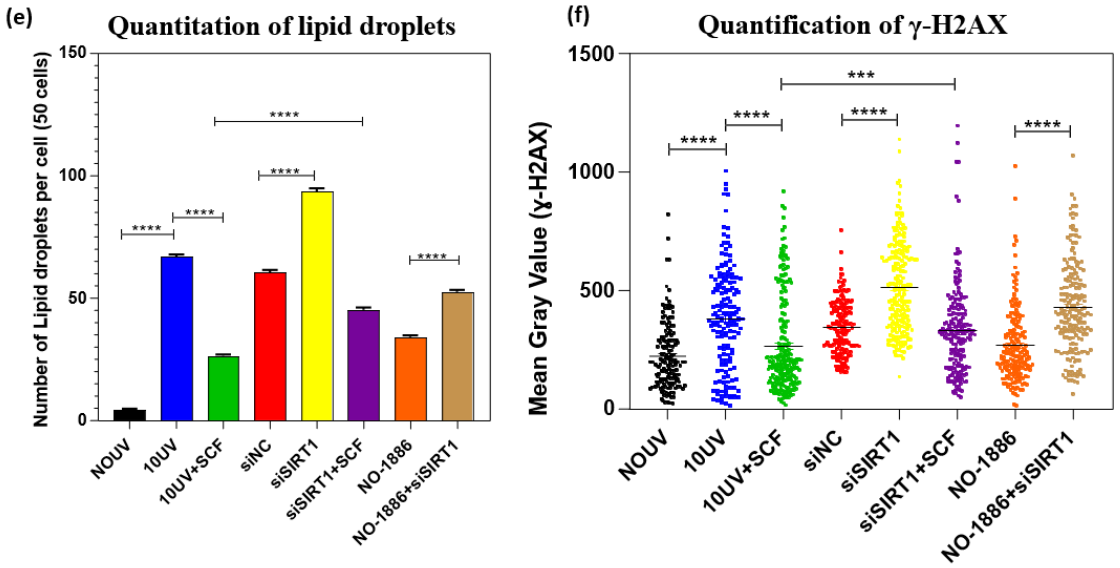

Figure 15 Reduced DNA damage upon SCF mediated SIRT1 treatment

Figure 15: SIRT1 represents the downstream effector protein in the SCF-LPL-SIRT1 signaling pathway

(a) Photomicrographs and (b) quantitation (count) of lipid droplets stained with Bodipy® in UV_B exposed NHEK treated with SCF, NO-1886 (LPL agonist), EX-527 (SIRT1 inhibitor) or co-treatment of Ex-527 with SCF/NO-1886 by confocal microscope (n=3). (c) Cyclobutane pyrimidine dimer (CPD) induction (ng/ml) in NHEK following treatment with SCF, NO-1886, Ex-527, or co-treatment of Ex-527 with SCF/NO-1886 in UV-B irradiated cells depicted as a bar graph (n=3). (d) Representative images depicting γ- H2AX staining (red) and lipid droplets (Bodipy® staining, green) in NHEK and (e) the quantitation (number) of lipid droplets and (f) γ-H2AX after treatment with various combinations of SCF, siLPL, siSIRT1 in UV-B irradiated NHEK using confocal microscope.

Together, our research proves that SCF induces LPL upregulation, which enhances lipolysis and protects keratinocytes against the toxic effects of UV-B, such as DNA damage, ROS production, mitochondrial damage by activating SIRT1, the terminal effector protein in the SCF-cKIT/LPL/SIRT1 signaling pathway.

Chapter 4: Conclusion

Genomic integrity is crucial for cell survival. Cells have therefore developed sophisticated mechanisms, such as DNA damage checkpoints and repair enzymes to safeguard their genome. Skin has also been endowed with a photoprotective barrier, melanin, to cope with the immense amount of chemical and environmental stress it is subjected to at all times. DNA photodamage is one of the most significant acute consequences of UVR. UVA (320 – 400 nm) and UVB (280 - 320 nm) exert various biological effects on the skin (Gilchrest, Eller et al. 1999). Since UV-B radiation is cytotoxic and mutagenic, and 3-4 orders of magnitude more efficient (J/cm2) than UVA in inducing DNA photodamage (Young, Chadwick et al. 1998) and skin cancer (de Gruijl 1995), we treated keratinocytes with UV-B radiation in our study. The findings of this study shed light on a novel protective mechanism in vitiligo keratinocytes, revealing that the stem cell factor (SCF) signaling pathway plays a crucial role in safeguarding these cells against UV-induced DNA damage. By activating lipoprotein lipase (LPL), SCF enhances lipid metabolism, which in turn leads to the upregulation of sirtuin 1 (SIRT1), a key protein involved in DNA repair and mitochondrial function. This intricate signaling axis SCF-LPL-SIRT1 demonstrates how keratinocytes can adapt and develop resilience in the absence of melanin, a pigment traditionally known for its protective properties against UV radiation. Our study not only highlights the critical role of lipid metabolism in maintaining genomic integrity but also provides an explanation for the paradoxically lower incidence of skin malignancies in individuals with vitiligo.

By showing that SCF reduces oxidative stress, prevents lipid peroxidation, and improves mitochondrial health, we establish a direct link between metabolic adaptation and cellular defense mechanisms. Mitochondria, being the powerhouses of the cell, play a crucial role in energy metabolism and cellular homeostasis. UV radiation is known to cause mitochondrial fragmentation and impair mitochondrial function, leading to increased ROS production and oxidative damage. Our findings indicate that SCF helps maintain mitochondrial integrity by preventing excessive fragmentation and promoting a healthier mitochondrial network. This suggests that SCF not only mitigates immediate UV-induced damage but also fosters long term metabolic resilience in keratinocytes, making it a promising target for therapeutic interventions.

The SCF-mediated decrease in mitochondrial lipid droplets and concurrent increase in mitochondrial tubulation indicated a central role of SCF in the uniform distribution of FAs

associated with lipid droplets within mitochondria for optimal -oxidation, particularly under stress conditions. We further explored the involvement of SCF mediated regulation of lipid metabolism in protecting against DNA damage. Since decreases in lipid droplets and TAGs indicated cellular lipases playing a role in mediating protection against UV-B damage. An increased UV-B caused DNA damage following treatment with orlistat, lipase inhibitor or its attenuation with NO-1886, a selective agonist of LPL (Niho, Mutoh et al. 2005) indicated LPL-mediated lipolysis to be a Significant protective mechanism in the modulation of UV responses in the skin. Our observation that treatment with Ex-527 or treatment with siSIRT1 was able to abrogate the protective action mediated by SCF or NO-1886, implicated SIRT1 to be the ultimate effector protein in SCF LPL-SIRT1 signaling. This discovery was concurrent with the prior established function of SIRT1 to mediate cell survival (Rajamohan, Pillai et al. 2009), stress modulation (Singh and Ubaid 2020), protection against UV-B induced DNA damage and keratinocyte differentiation (Brahmbhatt, Gupta et al. 2021).

The clinical validation of these findings, by showing increased expression of SCF and LPL in lesional vitiligo epidermis, strengthens the physiological relevance of such a pathway. These findings open up new therapeutic approaches that would promote skin resilience via targeted activation of SCF, LPL, and SIRT1. Applications might include topical or systemic strengthening of that pathway to reduce UV damage in patients with vitiligo or albinism or other conditions. Because lipid metabolism is an integral process tied to every cell signaling and stress response, any modulation of LPL activity could help protect against UV damage and other dermatological issues pertinent to oxidative stress and inflammation. This paradigm shift in the understanding of skin response to stress will be the foundation for manipulation with a metabolic reprogramming concept to obtain skin health and disease prevention. The identification of the SCF-LPL-SIRT1 axis demonstrates how intricately metabolism is interconnected with DNA repair and oxidative stress response in keratinocytes. Tapping into these findings may unfold new protective and rejuvenation avenues for skin research and could ultimately lead to breakthroughs in dermatological science.

References

1. Boer, M., Duchnik, E., Maleszka, R., & Marchlewicz, M. (2016). Structural and biophysical characteristics of human skin in maintaining proper epidermal barrier function. *Postepy dermatologii I alergologii*, *33*(1), 1–5. https://doi.org/10.5114/pdia.2015.48037
2. Yousef H, Alhajj M, Sharma S. Anatomy, Skin (Integument), Epidermis. [Updated 2022 Nov 14]. In: StatPearls [Internet]. Treasure Island (FL): StatPearls Publishing; 2024 Jan-. Available from: https://www.ncbi.nlm.nih.gov/books/NBK470464/
3. Hofmann E, Schwarz A, Fink J, Kamolz L-P, Kotzbeck P. Modelling the Complexity of Human Skin In Vitro. *Biomedicines*. 2023; 11(3):794. https://doi.org/10.3390/biomedicines11030794
4. Hirobe T. (2005). Role of keratinocyte-derived factors involved in regulating the proliferation and differentiation of mammalian epidermal melanocytes. *Pigment cell research*, *18*(1), 2–12. https://doi.org/10.1111/j.1600-0749.2004.00198.x
5. Misery, L. (2007). *How the skin reacts to environmental factors. Journal of the European Academy of Dermatology and Venereology, 21(s2), 5–8.* doi:10.1111/j.1468-3083.2007.02380.x
6. Landau, M. (2007). Exogenous Factors in Skin Aging. Current Problems in Dermatology, 1–13. doi:10.1159/000106405
7. Giglia-Mari, G., Zotter, A., & Vermeulen, W. (2010). *DNA Damage Response. Cold Spring Harbor Perspectives in Biology, 3(1), a000745–a000745*. doi:10.1101/cshperspect.a000
8. D'Orazio J, Jarrett S, Amaro-Ortiz A, Scott T. UV Radiation and the Skin. *International Journal of Molecular Sciences*. 2013; 14(6):12222-12248. https://doi.org/10.3390/ijms140612222
9. Chatterjee, N., & Walker, G. C. (2017). Mechanisms of DNA damage, repair, and mutagenesis. *Environmental and molecular mutagenesis*, *58*(5), 235–263. https://doi.org/10.1002/em.22087
10. Bhagavan, N. (2002). CHAPTER 24 – DNA Replication, Repair, and Mutagenesis, 545-562. https://doi.org/10.1016/B978-012095440-7/50026-3.
11. Hendi, Nagham & Elsakrmy, Noha & Ramotar, Dindial. (2021). The base excision repair process: comparison between higher and lower eukaryotes. Cellular and Molecular Life Sciences. 78. 10.1007/s00018-021-03990-9.

12. Lieber M. R. (2010). The mechanism of double-strand DNA break repair by the nonhomologous DNA end-joining pathway. *Annual review of biochemistry*, *79*, 181–211. https://doi.org/10.1146/annurev.biochem.052308.093131
13. Stinson, B. M., & Loparo, J. J. (2021). Repair of DNA Double-Strand Breaks by the Nonhomologous End Joining Pathway. *Annual review of biochemistry*, *90*, 137–164. https://doi.org/10.1146/annurev-biochem-080320-110356
14. Sconocchia, T., Foßelteder, J., Köhnke, T., Majeti, R., Reinisch, A. Engineering Oncogenic Heterozygous Gain-of-Function Mutations in Human Hematopoietic Stem and Progenitor Cells. J. Vis. Exp. (193), e64558, doi:10.3791/64558 (2023)
15. Scully, R., Panday, A., Elango, R. *et al.* DNA double-strand break repair-pathway choice in somatic mammalian cells. *Nat Rev Mol Cell Biol* **20**, 698–714 (2019). https://doi.org/10.1038/s41580-019-0152-0
16. Tiwari, V., Baptiste, B. A., Okur, M. N., & Bohr, V. A. (2021). Current and emerging roles of Cockayne syndrome group B (CSB) protein. *Nucleic acids research*, *49*(5), 2418–2434. https://doi.org/10.1093/nar/gkab085
17. Kciuk, M., Marciniak, B., Mojzych, M., & Kontek, R. (2020). Focus on UV-Induced DNA Damage and Repair-Disease Relevance and Protective Strategies. *International journal of molecular sciences*, *21*(19), 7264. https://doi.org/10.3390/ijms21197264
18. Le, L., Sirés-Campos, J., Raposo, G., Delevoye, C., & Marks, M. S. (2021). Melanosome Biogenesis in the Pigmentation of Mammalian Skin. *Integrative and comparative biology*, *61*(4), 1517–1545. https://doi.org/10.1093/icb/icab078
19. D'Mello, S. A., Finlay, G. J., Baguley, B. C., & Askarian-Amiri, M. E. (2016). Signaling Pathways in Melanogenesis. *International journal of molecular sciences*, *17*(7), 1144. https://doi.org/10.3390/ijms17071144
20. Wasmeier, C., Hume, A. N., Bolasco, G., & Seabra, M. C. (2008). Melanosomes at a glance. *Journal of cell science*, *121*(Pt 24), 3995–3999. https://doi.org/10.1242/jcs.040667
21. Hida, T., Kamiya, T., Kawakami, A., Ogino, J., Sohma, H., Uhara, H., & Jimbow, K. (2020). Elucidation of Melanogenesis Cascade for Identifying Pathophysiology and Therapeutic Approach of Pigmentary Disorders and Melanoma. *International journal of molecular sciences*, *21*(17), 6129. https://doi.org/10.3390/ijms21176129
22. Ebanks, J. P., Wickett, R. R., & Boissy, R. E. (2009). Mechanisms regulating skin pigmentation: the rise and fall of complexion coloration. *International journal of molecular sciences*, *10*(9), 4066–4087. https://doi.org/10.3390/ijms10094066

23. Cichorek, M., Wachulska, M., Stasiewicz, A., & Tymińska, A. (2013). Skin melanocytes: biology and development. *Postepy dermatologii i alergologii*, *30*(1), 30–41. https://doi.org/10.5114/pdia.2013.33376
24. Le, L., Sirés-Campos, J., Raposo, G., Delevoye, C., & Marks, M. S. (2021). Melanosome Biogenesis in the Pigmentation of Mammalian Skin. *Integrative and comparative biology*, *61*(4), 1517–1545. https://doi.org/10.1093/icb/icab078
25. D'Alba, L., & Shawkey, M. D. (2019). Melanosomes: Biogenesis, Properties, and Evolution of an Ancient Organelle. *Physiological reviews*, *99*(1), 1–19. https://doi.org/10.1152/physrev.00059.2017
26. Otręba, M., Miliński, M., Buszman E., et al. (2013). Hereditary hypomelanocytoses: the role of PAX3, SOX10, MITF, SNAI2, KIT, EDN3 and EDNRB genes. *Advances in Hygiene and Experimental Medicine*, 67(null), 1109-1118. https://doi.org/10.5604/17322693.1077722.
27. Suzukawa, A. A., Vieira, A., Winnischofer, S. M. B., Scalfo, A. C., Di Mascio, P., Ferreira, A. M. da C., … Martinez, G. R. (2012). *Novel properties of melanins include promotion of DNA strand breaks, impairment of repair, and reduced ability to damage DNA after quenching of singlet oxygen. Free Radical Biology and Medicine, 52(9), 1945–1953*. doi:10.1016/j.freeradbiomed.2012.02
28. Alikhan, A., Felsten, L. M., Daly, M., & Petronic-Rosic, V. (2011). Vitiligo: A comprehensive overview Part I: Introduction, epidemiology, quality of life, diagnosis, and work-up. *Journal of the American Academy of Dermatology*, *65*(3), 473-491. https://doi.org/10.1016/j.jaad.2010.11.061
29. Ezzedine, K., Eleftheriadou, V., Whitton, M., & van Geel, N. (2015). Vitiligo. *Lancet*, *386*(9988), 74-84. https://doi.org/10.1016/S0140-6736(14)60763-7
30. Jin, Y., Mailloux, C. M., Gowan, K., Riccardi, S. L., LaBerge, G., Bennett, D. C., ... & Spritz, R. A. (2010). NLRP1 is a vitiligo-associated gene. *American Journal of Human Genetics*, *86*(3), 356-360. https://doi.org/10.1016/j.ajhg.2010.02.006
31. Richmond, J. M., Bangari, D. S., Essien, K. I., Zhao, M., Hartnell, F. M., Gudjonsson, J. E., & Harris, J. E. (2017). Keratinocyte-derived chemokines orchestrate T cell positioning in vitiligo and may serve as biomarkers of disease. *Journal of Investigative Dermatology*, *137*(2), 350-358. https://doi.org/10.1016/j.jid.2016.10.026
32. Van den Boorn, J. G., Picavet, D. I., van Swieten, P. F., van Veen, H. A., Konijnenberg, D., van der Veen, J. P., ... & Luiten, R. M. (2011). Skin-depigmenting agent monobenzone induces potent T cell autoimmunity toward pigmented cells by tyrosinase haptenation and

melanosome autophagy. *Journal of Clinical Investigation*, *121*(10), 3830-3841. https://doi.org/10.1172/JCI45017

33. Wang, X., Du, J., Wang, T., Sun, Y., Wang, X., & Dong, L. (2018). Role of oxidative stress in vitiligo: A review. *Journal of Dermatological Science*, *92*(1), 8-14. https://doi.org/10.1016/j.jdermsci.2018.06.003
34. Harris, J. E., & Rashighi, M. (2020). The pathophysiology of vitiligo. *Autoimmunity*, *53*(1), 57-65. https://doi.org/10.1080/08916934.2019.1680917
35. Ashman, L. K. (1999). The biology of stem cell factor and its receptor c-KIT. *International Journal of Biochemistry & Cell Biology*, *31*(10), 1037–1051. https://doi.org/10.1016/S1357-2725(99)00062-8
36. Caruana, G., & Sukhdeo, K. (2021). The role of SCF/c-KIT signaling in epidermal homeostasis and repair. *Journal of Dermatological Science*, *103*(2), 95–106. https://doi.org/10.1016/j.jdermsci.2021.04.003
37. Hirota, S., Isozaki, K., Moriyama, Y., Hashimoto, K., Nishida, T., Ishiguro, S., ... & Kitamura, Y. (1998). Gain-of-function mutations of c-KIT in human gastrointestinal stromal tumors. *Science*, *279*(5350), 577–580. https://doi.org/10.1126/science.279.5350.577
38. Jian, Z., Li, K., Liu, L., Zhang, Y., Zhou, L., Li, C., & Wu, X. (2014). SCF/c-KIT signaling promotes keratinocyte proliferation, migration, and protects against UV-induced apoptosis. *Experimental Dermatology*, *23*(1), 20–25. https://doi.org/10.1111/exd.12299
39. Lennartsson, J., & Rönnstrand, L. (2012). The stem cell factor receptor/c-KIT as a drug target in cancer. *Current Cancer Drug Targets*, *12*(5), 429–444. https://doi.org/10.2174/156800912800672344
40. Mol, C. D., Dougan, D. R., Schneider, T. R., Skene, R. J., Kraus, M. L., Scheibe, D. N., ... & Swenson, L. (2003). Structural basis for the autoinhibition and STI-571 inhibition of c-KIT tyrosine kinase. *Journal of Biological Chemistry*, *278*(34), 31461–31464. https://doi.org/10.1074/jbc.M304563200
41. Roskoski, R. (2005). Structure and regulation of c-KIT protein-tyrosine kinase—the stem cell factor receptor. *Biochemical and Biophysical Research Communications*, *338*(3), 1307–1315. https://doi.org/10.1016/j.bbrc.2005.10.003
42. Rothschild, G., Bernheimer, H., & Goldstein, M. (2001). Membrane-bound vs. soluble SCF: Implications in cell survival and differentiation. *Journal of Cellular Signaling*, *16*(4), 455–467.

43. Zhang, Y., Wang, H., Liu, J., Zhang, Y., Liu, W., & Wu, X. (2018). c-KIT signaling modulates keratinocyte survival and differentiation during skin repair. *Molecular Cell Research*, *1865*(7), 1351–1362. https://doi.org/10.1016/j.bbamcr.2018.02.007
44. Grabowska, W., Sikora, E., & Bielak-Zmijewska, A. (2017). Sirtuins, a promising target in slowing down the ageing process. *Biogerontology*, *18*(4), 447–476. https://doi.org/10.1007/s10522-017-9685-9
45. Vassilopoulos, A., Fritz, K. S., Petersen, D. R., & Gius, D. (2011). The human sirtuin family: evolutionary divergences and functions. *Human genomics*, *5*(5), 485–496. https://doi.org/10.1186/1479-7364-5-5-485
46. Yuan, H., & Marmorstein, R. (2012). Structural basis for sirtuin activity and inhibition. *The Journal of biological chemistry*, *287*(51), 42428–42435. https://doi.org/10.1074/jbc.R112.372300
47. Zhang, J., Xiang, H., Liu, J., Chen, Y., He, R. R., & Liu, B. (2020). Mitochondrial Sirtuin 3: New emerging biological function and therapeutic target. *Theranostics*, *10*(18), 8315–8342. https://doi.org/10.7150/thno.45922
48. Teixeira CSS, Cerqueira NMFSA, Gomes P, Sousa SF. A Molecular Perspective on Sirtuin Activity. *International Journal of Molecular Sciences*. 2020; 21(22):8609. https://doi.org/10.3390/ijms21228609
49. Davenport, A. M., Huber, F. M., & Hoelz, A. (2014). Structural and functional analysis of human SIRT1. *Journal of molecular biology*, *426*(3), 526–541. https://doi.org/10.1016/j.jmb.2013.10.009
50. Zhang T, Kraus WL. SIRT1-dependent regulation of chromatin and transcription: linking NAD (+) metabolism and signaling to the control of cellular functions. Biochim Biophys Acta. 2010 Aug;1804(8):1666-75. doi: 10.1016/j.bbapap.2009.10.022. Epub 2009 Oct 30. PMID: 19879981; PMCID: PMC2886162.
51. Iside C, Scafuro M, Nebbioso A, Altucci L. SIRT1 Activation by Natural Phytochemicals: An Overview. Front Pharmacol. 2020 Aug 7;11:1225. doi: 10.3389/fphar.2020.01225. PMID: 32848804; PMCID: PMC7426493.
52. Yuan Y, Cruzat VF, Newsholme P, Cheng J, Chen Y, Lu Y. Regulation of SIRT1 in aging: Roles in mitochondrial function and biogenesis. Mech Ageing Dev. 2016 Apr;155:10-21. doi: 10.1016/j.mad.2016.02.003. Epub 2016 Mar 7. PMID: 26923269.
53. Kwon HS, Ott M. The ups and downs of SIRT1. Trends Biochem Sci. 2008 Nov;33(11):517-25. doi: 10.1016/j.tibs.2008.08.001. Epub 2008 Sep 18. PMID: 18805010.

54. Alves-Fernandes, D. K., & Jasiulionis, M. G. (2019). The Role of SIRT1 on DNA Damage Response and Epigenetic Alterations in Cancer. *International journal of molecular sciences*, *20*(13), 3153. https://doi.org/10.3390/ijms20133153
55. Chung, S., Yao, H., Caito, S., Hwang, J. W., Arunachalam, G., & Rahman, I. (2010). Regulation of SIRT1 in cellular functions: role of polyphenols. *Archives of biochemistry and biophysics*, *501*(1), 79–90. https://doi.org/10.1016/j.abb.2010.05.003
56. Chen, A.C.H.; Peng, Q.; Fong, S.W.; Lee, K.C.; Yeung, W.S.B.; Lee, Y.L. DNA Damage Response and Cell Cycle Regulation in Pluripotent Stem Cells. Genes 2021, 12, 1548. https://doi.org/10.3390/genes12101548
57. Ozawa, Yoko & Kubota, Shunsuke & Narimatsu, Toshio & Yuki, Kenya & Koto, Takashi & Sasaki, Mariko & Tsubota, Kazuo. (2010). Retinal Aging and Sirtuins. Ophthalmic research. 44. 199-203. 10.1159/000316484.
58. Motta MC, Divecha N, Lemieux M, Kamel C, Chen D, Gu W, Bultsma Y, McBurney M, Guarente L. Mammalian SIRT1 represses forkhead transcription factors. Cell. 2004 Feb 20;116(4):551-63. doi: 10.1016/s0092-8674(04)00126-6. PMID: 14980222.
59. Yang Y, Hou H, Haller EM, Nicosia SV, Bai W. Suppression of FOXO1 activity by FHL2 through SIRT1-mediated deacetylation. EMBO J. 2005 Mar 9;24(5):1021-32. doi: 10.1038/sj.emboj.7600570. Epub 2005 Feb 3. PMID: 15692560; PMCID: PMC554122.
60. Lee, Y. L., Peng, Q., Fong, S. W., Chen, A. C., Lee, K. F., Ng, E. H., Nagy, A., & Yeung, W. S. (2012). Sirtuin 1 facilitates generation of induced pluripotent stem cells from mouse embryonic fibroblasts through the miR-34a and p53 pathways. *PloS one*, *7*(9), e45633. https://doi.org/10.1371/journal.pone.0045633

Supplementary Figures

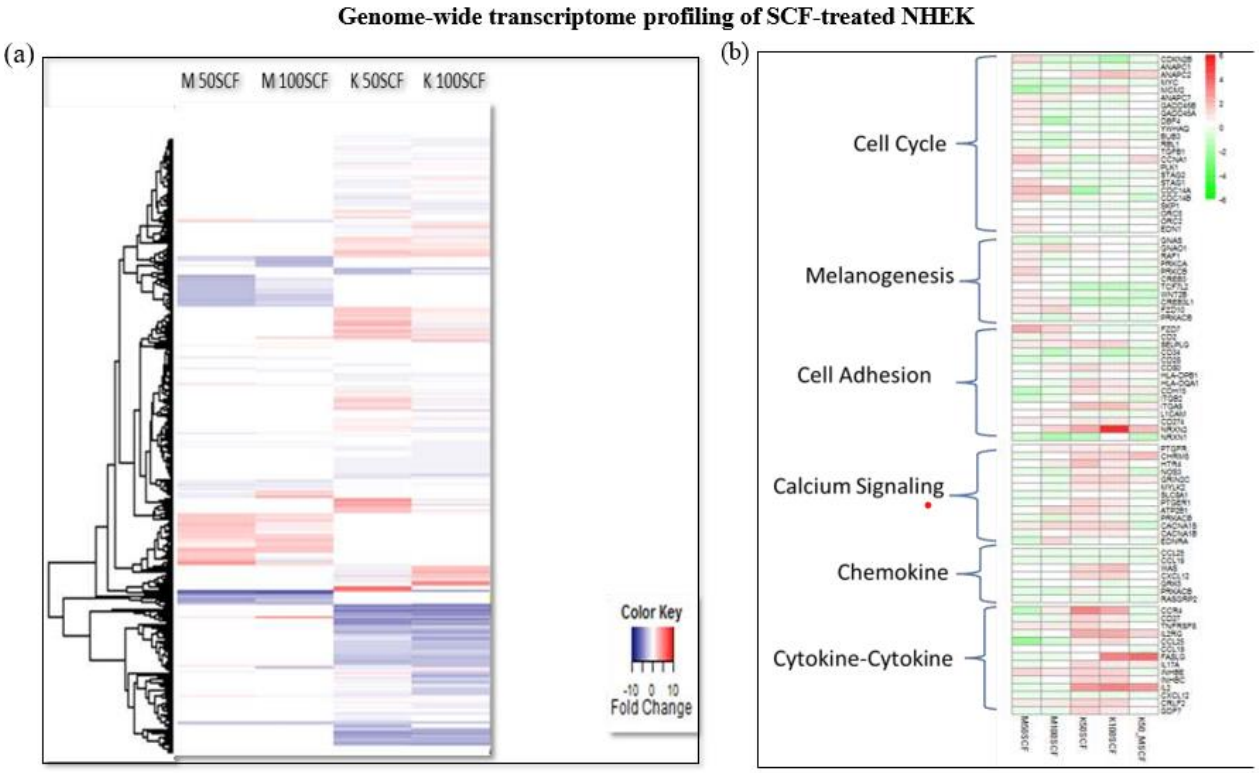

Supplementary Figure S1: **(a)** Genome-wide transcriptome profiling of primary melanocytes (M) and keratinocytes (K) treated with recombinant human SCF (50ng/ml, 100ng/ml; 48 hours) showing distinct transcriptional regulation in melanocytes and keratinocytes. **(b)** Transcriptional regulation of genes involved in cell cycle, melanogenesis, cell adhesion, calcium signaling and cytokine-cytokine signaling is depicted as a heat map in SCF-treated melanocytes and keratinocytes

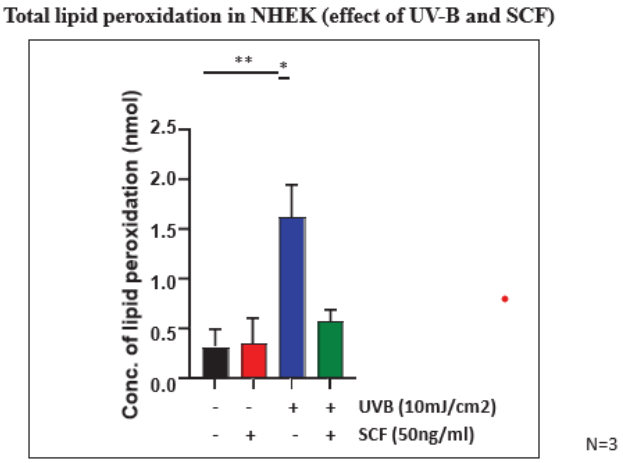

Supplementary Figure S2: Bar graph showing lipid peroxidation levels in NHEK upon treatment with SCF in absence or presence of 10mJ/cm^2 UV-B radiation (n=3). Lipid peroxidation is represented in nmol.

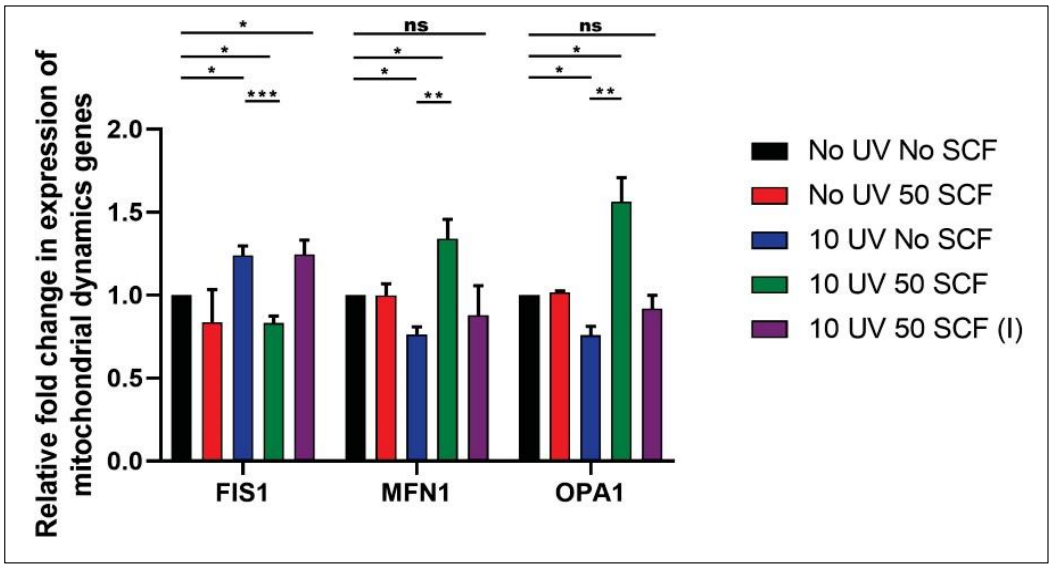

Supplementary Figure S3: Expression of different mitochondrial fission (FIS1) and fusion (OPA1 and MFN1) transcripts using real time PCR. SYBR Green chemistry was used as a detection system. Data was normalized using 18s rRNA (n=3, *P<0.05, **P<0.01, ***P<0.001).

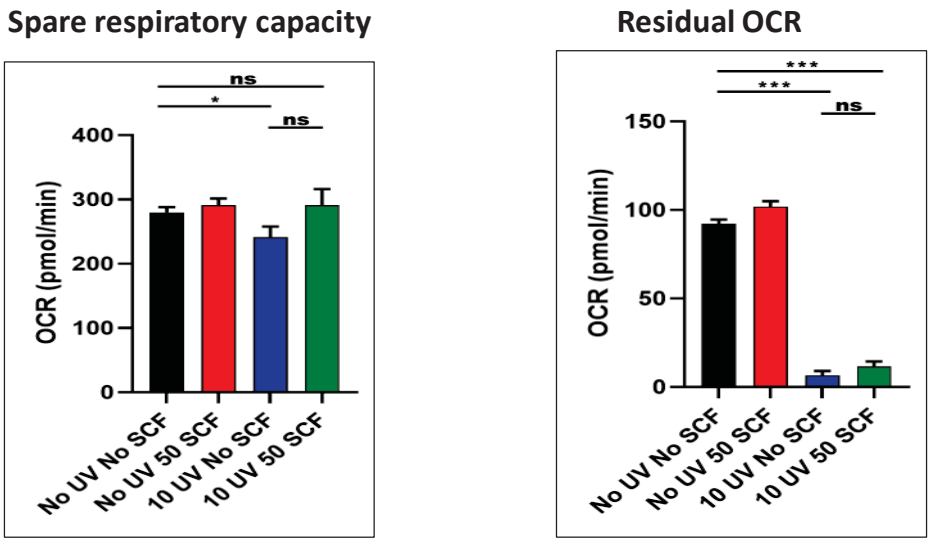

Supplementary Figure S4: Oxygen consumption rate (OCR) in pmol/min was determined after different mitochondrial complex inhibitors addition using Agilent Seahorse instrument in NHEK cells (n=3, *P<0.05, **P<0.01, ***P<0.001).

Ultrastructural studies of lipid droplet-mitochondria interaction in UV-B irradiated keratinocytes

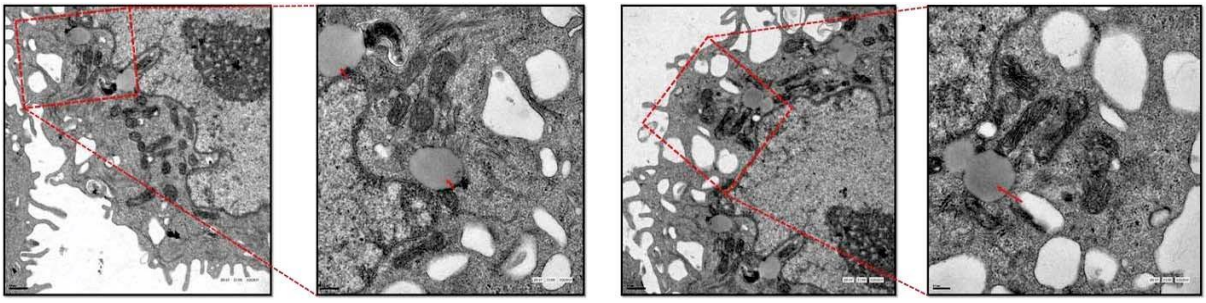

Supplementary Figure S5: Transmission electron microscopy images showing close physical interaction between lipid droplets and mitochondria in UV-B irradiated cells. Red arrows indicate lipid droplets.

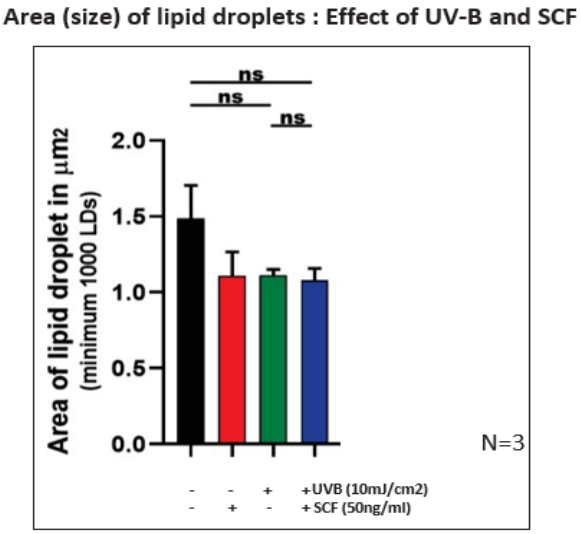

Supplementary Figure S6: Quantitation (size) of lipid droplets visualized by Bodipy® staining in cells treated with or without UV-B in presence or absence of SCF using confocal microscope.

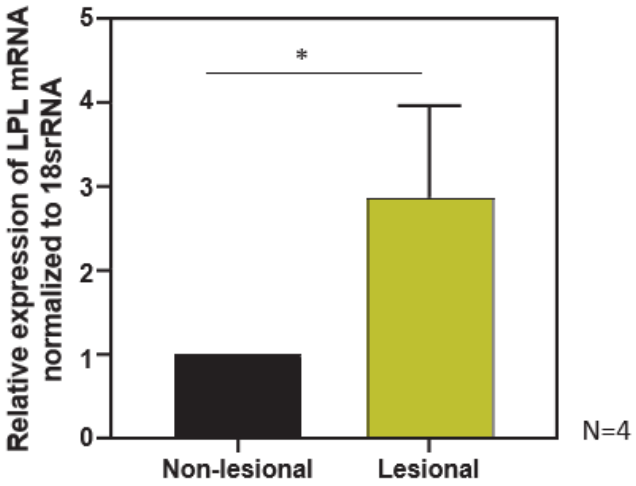

Supplementary Figure S7: Bar graph showing transcript levels of LPL in epidermis samples of lesional and non-lesional skin from 4 vitiligo patients. Data was normalized using 18s rRNA (n=4, *P<0.05).

Immunocytochemistry of γ-H2AX in NHEK (effect of orlistat and NO-1886 on UV-B mediated DNA damage)

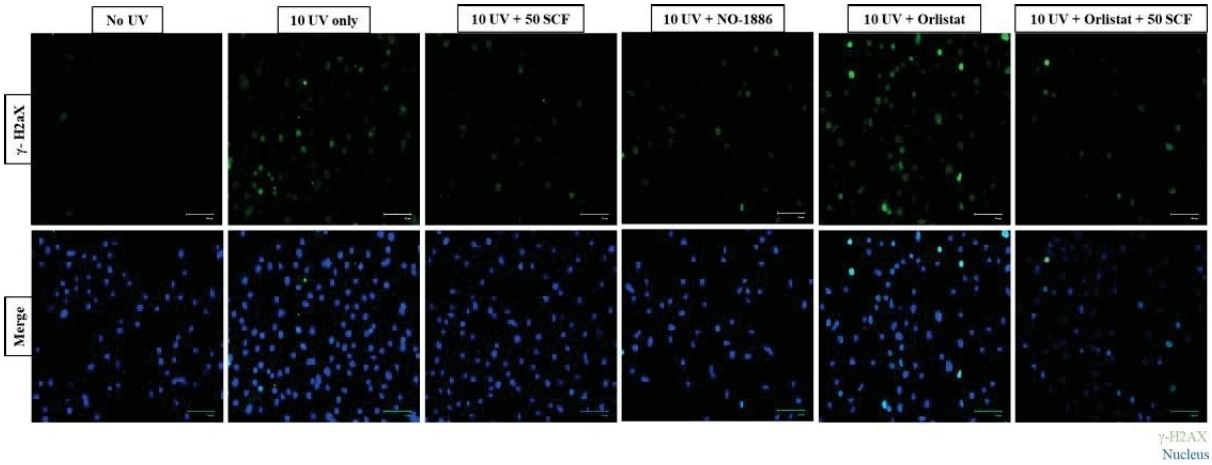

Supplementary Figure S8: γ-H2AX staining intensity (green) in NHEK cells upon treatment with different combinations of SCF, NO-1886, orlistat, or a combination of SCF and orlistat in UV-B exposed cells. (n=3)

Cyclobutane pyrimidine dimer (CPD) assay in NHEK (effect of orlistat and NO-1886 on UV-B mediated DNA damage)

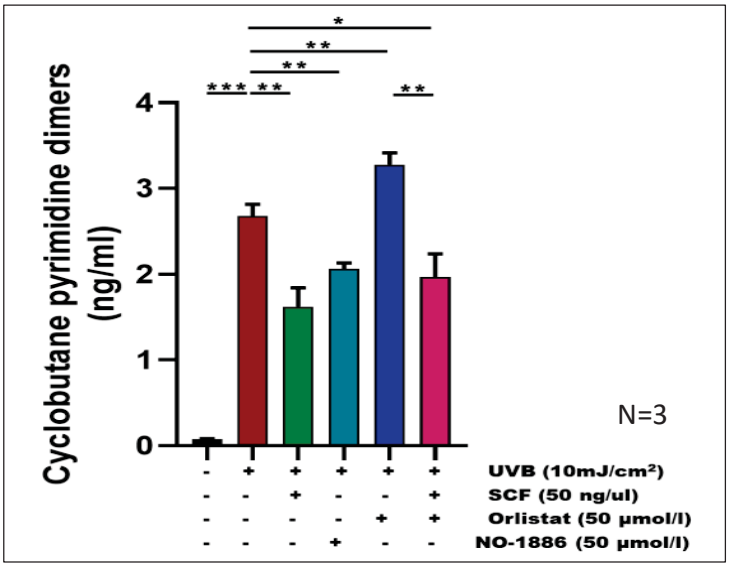

Supplementary Figure S9: Cyclobutane pyrimidine dimer (CPD) formation (ng/ml) in NHEK upon treatment with different combinations of SCF, NO-1886 and orlistat in UV-B irradiated cells plotted as a bar graph (n=3).

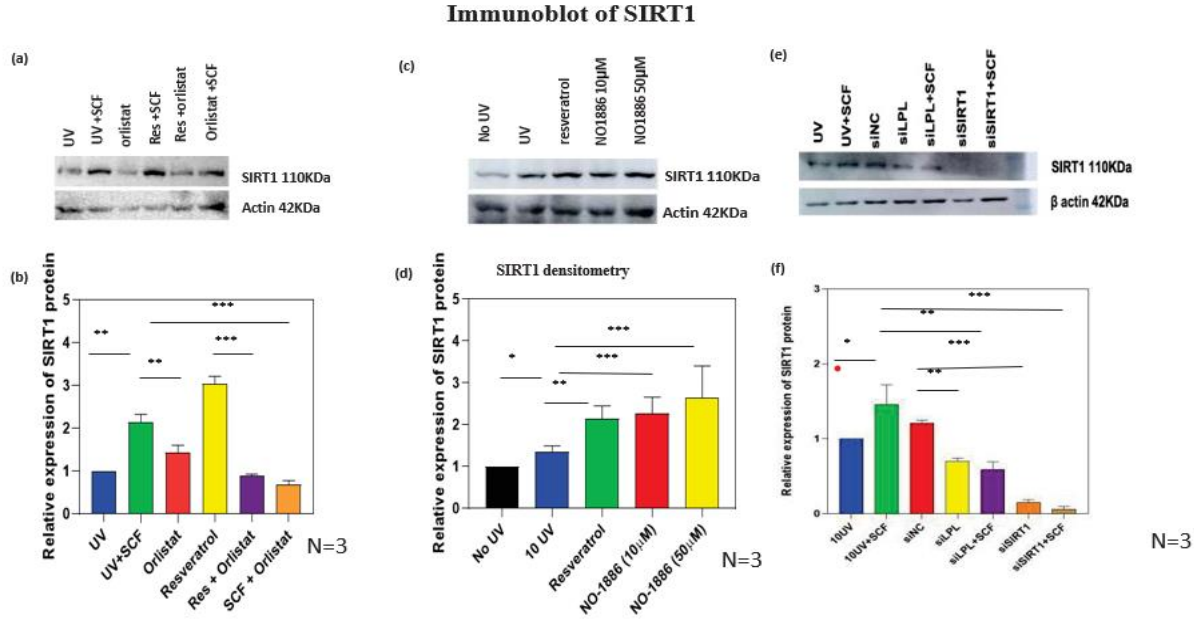

Supplementary Figure S10: Western blot showing expression of SIRT1 protein upon treatment of UV_B irradiated keratinocytes upon treatment with **(a)** SCF and orlistat **(c)** NO-1886, **(e)** siLPL and siSIRT1 and their respective **(b, d, f)** Densitometry (n=3). β-actin was taken as an internal control for all western blot experiments.

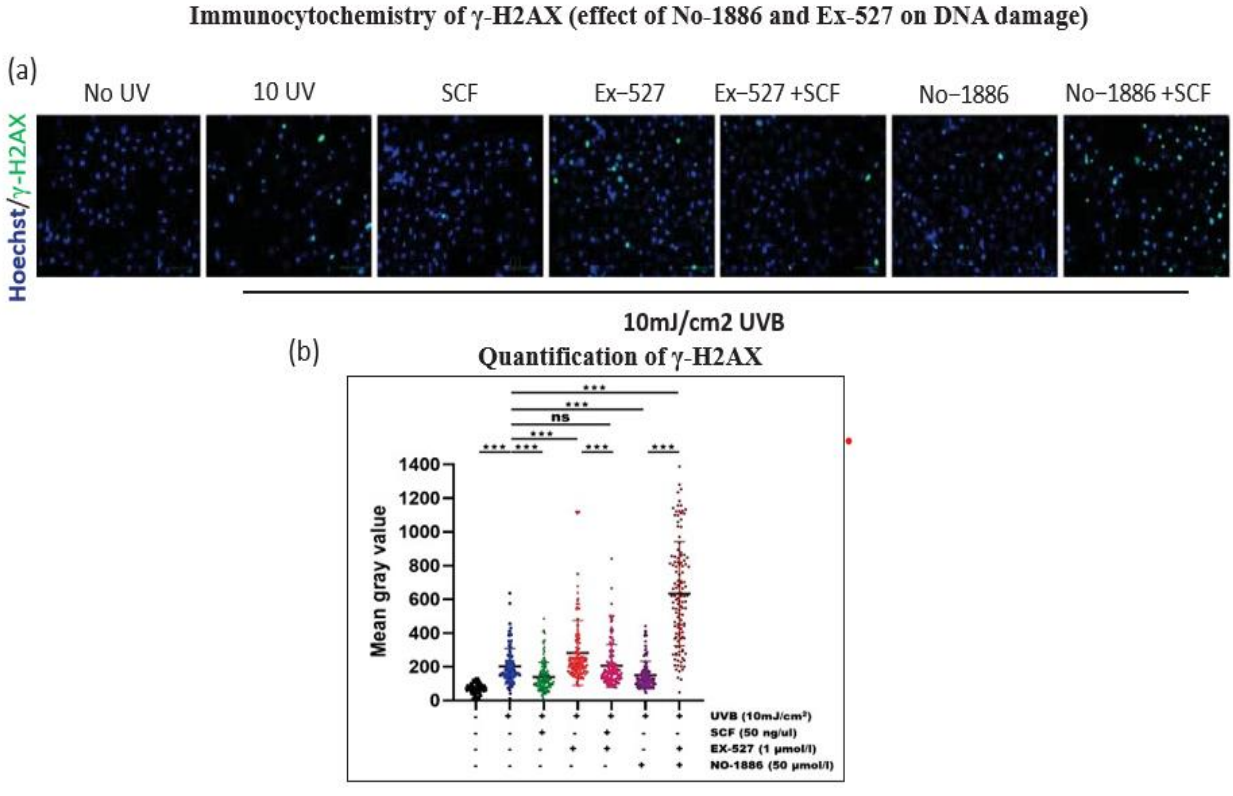

Supplementary Figure S11: γ-H2AX staining intensity (green) in NHEK upon treatment SCF, NO-1886, Ex-527, or a combination of Ex-527 and SCF/NO-1886 in UV-B irradiated cells plotted as a bar graph (n=3).

Cyclobutane pyrimidine dimer (CPD) assay (effect of Ex-527 and NO-1886on DNA damage)

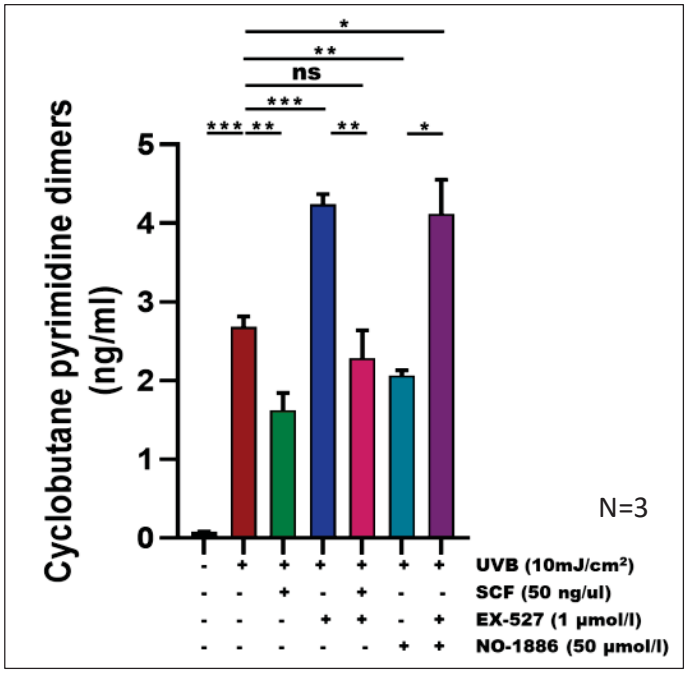

Supplementary Figure S12: Cyclobutane pyrimidine dimer (CPD) formation (ng/ml) in NHEK upon treatment SCF, NO-1886, Ex-527, or a combination of Ex-527 and SCF/NO- 1886 in UV-B irradiated cells plotted as a bar graph (n=3).